Self-Assembly of Luminescent Alkynyl-Based Platinum-Cadmium Complexes Containing Auxiliary Diimine or Terpyridine Ligands.

Jesús R. Berenguer,*[†] Belén Gil,[†] Julio Fernández,[†] Juan Forniés,[‡] and Elena Lalinde*[†]

Departamento de Química-Grupo de Síntesis Química de La Rioja, UA-CSIC, Universidad de La Rioja, 26006, Logroño, Spain. Departamento de Química Inorgánica, Instituto de Ciencia de Materiales de Aragón, Universidad de Zaragoza-Consejo Superior de Investigaciones Científicas, 50009 Zaragoza, Spain.

Abstract

Reaction of different "Cd(N-N)$_2$$^{2+}$" (N-N = bpy, dmbpy, phen) or "Cd(trpy)$^{2+}$" fragments with *cis*- or *trans*- (**5**) dianionic bis(alkynyl) platinate substrates [Pt(C$_6$F$_5$)$_2$(C≡CR)$_2$]$^{2-}$ (R = Ph **a**, Tol **b**) leads to the generation of novel bimetallic neutral Platinum-Cadmium derivatives, which show photoluminescence (PL) strongly influenced by the structure and the media. In complexes [*cis*-Pt(C$_6$F$_5$)$_2$(C≡CR)$_2$Cd(N-N)$_2$] (N-N = bpy (**1**), dmbpy (**2**), phen (**3**)), the dianionic *cis*-bis(alkynyl) platinate fragment interacts with the "Cd(N-N)$_2$$^{+2}$" unit mainly through both the C$_\alpha$ atoms (d(Cd-C$_\alpha$) = 2.417(5)-2.554(5) Å) and the Pt center (d(Pt-Cd) ~ 3.10 Å); while in complexes [*cis*-Pt(C$_6$F$_5$)$_2$(C≡CR)$_2$Cd(trpy)] (**4**), probably due to the presence of only three Cd-N bonds, the Pt-Cd interaction is enhanced (d(Pt-Cd) ~ 3.00 Å), the Cd(II) atom being additionally solvated with acetone or H$_2$O. By contrast, in complexes [*trans*-Pt(C$_6$F$_5$)$_2$(C≡CR)$_2$Cd(bpy)$_2$] (**6**) the Cd center is found to be in a distorted trigonal-bipyramid coordination, interacting with one of the Pt-C$_\alpha$ bonds of the platina-bis(alkynyl) unit with very short Cd-C$_\alpha$ (2.372(10) Å) and Pt-Cd (2.8966(6) Å) bond

distances. Bimetallic complexes **1** – **4**, having *cis*-configured platinum fragments, exhibit, in solid state, blue and/or green phosphorescence with contribution of close emissive states of different natures: metal (Pt, Cd) perturbed ππ* intraligand (alkynyl, polyimine) manifolds mixed, to a greater (trpy complexes **4**) or lesser extend, with (Pt-Cd) charge transfer (MM′CT). In glassy state (2-MeTHF, 77 K), complexes **1b** – **4b** exhibit structured emissions mainly ascribed to (diimine **1b** – **3b**, trpy **4b**) ^{3}ππ phosphorescence, likely mixed with some ligand (alkyne) to ligand (imine) charge transfer (^{3}LL'CT). Complexes **6** are not emissive in solid state at room temperature. At 77 K they display a high energy ^{3}IL/^{3}MLCT (L = C≡CR) blue-shifted emission relative to **5** and, in the case of **6b**, an additional low energy feature, tentatively ascribed to ππ stacking interactions, in accordance with the presence of very short π···π contacts (3.25 Å) found in the extended lattice of **6b**.

Introduction

There is a growing interest in luminescent metal complexes because of their potential application in molecular electronic and material science.[1-11] Within this field, alkynyl metal complexes represent an active area of interest with manifold emissive origins depending on the structural features as well as on the nature of the metal, alkynyl substituents and coligands.[12-21] In particular, it is now widely recognized that the propensity for metalophillic interactions in d^{10} (Cu^I, Ag^I, Au^I, Hg^{II}) and d^8 (Pt^{II}) alkynyl compounds determines their solid state structures and plays a key role in their luminescent properties. [12-22] Furthermore, the potentially bridging character of the alkynyl ligands, either through the electron density of the C≡C units or by using internal or terminal polypyridyl-functionalized alkynyl entities, makes them ideal groups for

design multi-component or heterometallic complexes that usually exhibit more efficient long-lived and often dual photoluminescence with wider ranges of colors.[15,23-30]

Within this field, although considerable work has been carried out on alkynyl compounds in relation with d^{10} (group 11 and Hg^{II}) metals,[7,12,15,21,22,25-39] relatively few studies have explored the chemistry of homo[40-43] and heteropolynuclear d^{10}-cadmium(II) alkynyl systems[44-47] and little is known about their photophysical behavior.[44-47] In view of this fact and given the recent interest in complexes containing unusual $Pt^{II} \rightarrow Cd^{II}$ donor-acceptor bonds,[45,46,48-51] we have been involved in examining the reactivity of anionic alkynyl platinates towards Cd^{II} salts, with the aim of synthetizing photoluminescent heteropolynuclear complexes stabilized by either $\eta^2 \cdots Cd \cdots$alkynyl and/or Pt-Cd bonding interactions.[44-47] We have found that the degree of interaction of Cd^{II} with the alkynyl entities and the basic platinum center seems to be modulated by the number and nature of the ligands around the divalent Cd^{II}.

Thus, the first documented Cd^{II} alkynyl complexation was reported in the tetranuclear sandwich-type anionic cluster $[\{Pt(C \equiv CPh)\}_2(CdCl)_2]^{2-}$ (**A**, chart 1), stabilized by eight μ-η^1-alkynyl and four short $Pt \cdots Cd$ bonding interactions. This cluster (**A**) containing cationic "CdCl$^+$" units was generated, together with the 1:2 adduct $[\{Pt(C \equiv CPh)_4\}(CdCl_2)_2]^{2-}$ (**B**, chart 1) having neutral $CdCl_2$ entities and μ-η^2-alkynyl$\cdots$Cd interactions, by reaction of $[Pt(C \equiv CPh)_4]^{2-}$ with $CdCl_2$ (1:2 molar ratio).[44] Furthermore, the mixed platinates $[cis\text{-}Pt(C_6F_5)_2(C \equiv CR)_2]^{2-}$ are able to stabilize, through η^2 alkyne interactions, not only the neutral $CdCl_2$ unit (**C**, chart 1), but also a naked Cd^{II} (**D**, chart 1), the latter by reaction with $Cd(ClO_4)_2$ regardless of the molar ratio used.[47] Curiously, if the reaction takes place in the presence of cyclen (1,4,7,10-tetraazacyclodecane) the platinum center effectively competes with the alkynyl ligands, affording an unusual bimetallic derivative (**E**, chart 1) containing a very short Pt-Cd

bond (2.764(1) Å) and retaining only a weak interaction with one of the alkynyl fragments.[46] These results prompted us to investigate the coordination of the alkynyl platinates *cis-* and *trans-*$[Pt(C_6F_5)_2(C{\equiv}CR)_2]^{2-}$ (R = Ph, Tol) towards Cd^{II} in the presence of stronger chelating polyimine ligands such as 2,2′-bipyridine (bpy), 5,5′-dimethyl-2,2′-bipyridine (dmbpy), 1,10-phenanthroline (phen) and 2,2′,6′,2′′-terpyridine (trpy). We note that these ligands have been widely used for the synthesis of coordination complexes,[52-54] and also supramolecular structures,[55-57] with interesting photoluminescence properties.[6]

In this paper we describe the synthesis, characterization and photophysical properties of a family of unusual bimetallic complexes $[cis-Pt(C_6F_5)_2(C{\equiv}CR)_2Cd(N-N)_2]$ (R = Ph, Tol; N-N = bpy, dmbpy, phen), $[cis-Pt(C_6F_5)_2(C{\equiv}CR)_2Cd(trpy)]$ (R = Ph, Tol) and $[trans-Pt(C_6F_5)_2(C{\equiv}CR)_2Cd(bpy)_2]$.

Experimental Section

Materials: Complete details concerning the synthesis and spectroscopic characterization of the complexes **1 − 6** are provided as Supporting Information. All reactions and manipulations were carried out under argon atmosphere using distilled solvents, purified by known procedures. $(PMePh_3)_2[cis-Pt(C_6F_5)_2(C{\equiv}CR)_2]$ (R = Ph,[58] Tol[47]) and $(NBu_4)_2[trans-Pt(C_6F_5)_2(C{\equiv}CPh)_2]$[59] were prepared according to literature procedures. Other reagents such as 2,2′-bipyridine (bpy), 5,5′-dimethyl-2,2′-bipyridine (dmbpy), 1,10-phenantroline (phen) and 2,2′,6′,2′′-terpyridine (trpy) were obtained from commercial sources.

X-ray Crystallography. Details of the structural analyses for all complexes are summarized in Table 1. Colorless crystals of **1a** and **3a** were obtained by slow diffusion of a solution of $Cd(ClO_4)_2 \cdot 6H_2O$ (~ 4 mg) in acetone into a solution of $(PMePh_3)_2[cis-$

Pt(C$_6$F$_5$)$_2$(C≡CPh)$_2$] (12 mg) and the N-N ligand (4 mg, bpy **1a**; phen **3a**) also in acetone at room temperature. For complex **2a** and **6b** yellow crystals were obtained by cooling (- 30 ºC) saturated solutions of the corresponding crude solids in acetone. Colorless or yellow crystals of **4a** or **4b**, respectively, were obtained by slow diffusion of n-hexane (**4a**) or isopropilether (**4b**) into the respective solutions of the complexes in acetone. One (**1a**, **3a**) or two (**4a**, **6b**) molecules of acetone, one molecule of acetone and 0.75 of water (**2a**) or three molecules of acetone and one of water (**4b**) were found in the corresponding asymmetric units. X-ray intensity data were collected with a NONIUS-κCCD area-detector diffractometer, using graphite-monochromated Mo-K$_\alpha$ radiation. Images were processed using the DENZO and SCALEPACK suite of programs[60] and the structures were solved by Direct Methods using SHELXS-97 (**2a**, **4b**)[61] or Patterson and Fourier methods using DIRDIF92 (**1a**, **3a**, **4a**, **6b**).[62] The absorption corrections were performed using SORTAV[63] (**1a**, **2a**, **3a**, **4a**, **6b**) or XABS2[64] (**4b**).The structures were refined by full-matrix least squares on F^2 with SHELXL-97[61] and all non-hydrogen atoms were assigned anisotropic displacement parameters. The hydrogen atoms were constrained to idealized geometries fixing isotropic displacement parameters 1.2 times the U$_{iso}$ value of their attached carbon for the aromatic and 1.5 times for the methyl groups. For complex **6b**, which crystallizes in the non-centrosymmetric space group *Cc*, the crystal chosen for this structural analysis was found to be an inversion twin with occupancy 0.249(6) for the second component. Several restraints have been used to model one acetone molecule in **2a**, **4b** and **6b**. Finally, all the structures present some residual peaks greater than 1 e Å^{-3} in the vicinity of the metal atoms (or the crystallization solvent for **4b**), but with no chemical meaning.

Results and Discussion

Synthesis and Characterization. As shown in Scheme 1 (i), treatment of $(PMePh_3)_2[cis\text{-}Pt(C_6F_5)_2(C\equiv CR)_2]$ (R = Ph **a**, Tol **b**) with $Cd(ClO_4)_2\cdot 6H_2O$ and two equivalents of diimine ligand (bpy, dmbpy, phen) in acetone affords the bimetallic neutral Platinum-Cadmium complexes $[cis\text{-}Pt(C_6F_5)_2(C\equiv CR)_2Cd(N\text{-}N)_2]$ (N-N = bpy (**1**), dmbpy (**2**), phen (**3**)) as pale yellow or white (**2b**) solids in moderate yields (43-62 %). It is noteworthy that the same products are obtained using only one equivalent of diimine ligands, but in lower yields. Similarly, the reaction of $(PMePh_3)_2[cis\text{-}Pt(C_6F_5)_2(C\equiv CR)_2]$ with $Cd(ClO_4)_2\cdot 6H_2O$ in the presence of the tridentate $2,2',6',2''$-terpyridine (trpy) ligand gives rise to the corresponding bimetallic neutral complexes $[cis\text{-}Pt(C_6F_5)_2(C\equiv CR)_2Cd(trpy)]$ (R = Ph **4a**, Tol **4b**, Scheme 1, ii) as pale yellow (**4a**) or white (**4b**) solids. For both derivatives colorless crystals suitable for X-ray studies were obtained by slow diffusion of n-hexane (**4a**) or isopropylether (**4b**) into saturated solutions of the crude solids in acetone. As can be observed in Figures 2 (**4a**) and 3 (**4b**), in both cases the "*in situ*" generated dicationic "Cd(trpy)$^{+2}$" unit captures a solvent molecule (acetone **4a**; acetone or H_2O **4b**) to give a 6-coordinate environment upon coordination to the corresponding bis(alkynyl) platinate fragment. However, we noted that in both cases the crystals lost the solvent acetone molecules easily in contact with air.

We have recently found that the $[trans\text{-}Pt(C_6F_5)_2(CN)_2]^{2-}$ dianionic isomer exhibits a greater tendency to form Pt-Tl bonds than the corresponding *cis*- one.[65] Thus, we considered it of interest to explore the behavior of the related $[trans\text{-}Pt(C_6F_5)_2(C\equiv CR)_2]^{2-}$ (R = Ph **5a**,[59] Tol **5b**) towards the "in situ" generated "Cd(bpy)$_2$$^{+2}$" unit. The precursor $(NBu_4)_2[trans\text{-}Pt(C_6F_5)_2(C\equiv CTol)_2]$ **5b** has been prepared with this aim, following a similar synthetic procedure to that previously reported for the

phenylethynyl derivative[59] (see experimental for details and characterization). As shown in scheme 1 (iii), the use of the corresponding *trans*- isomers as precursors in the analogous reactions with $Cd(bpy)_2^{+2}$ in acetone affords the bimetallic neutral derivatives [*trans*-$Pt(C_6F_5)_2(C\equiv CR)_2Cd(bpy)_2$] (R = Ph **6a**, Tol **6b**) as a white (**6a**) or a bright yellow solid (**6b**) in moderate yields (62 % **6a**, 45 % **6b**).

All **1** − **4**, **6** complexes are air and moisture stable solids and were characterized by elemental analysis, conductivities, MASS spectrometry and IR and NMR spectroscopy. In particular, we noted that once isolated the phenylethynyl derivatives (**1a** - **4a, 6a**) are insoluble in common organic solvents, except in acetone in which they are soluble enough to record the corresponding ^1H and ^{19}F NMR spectra, but not for conductivity measurements (see experimental). In addition, single crystal X-ray diffraction studies have been carried out for **1a** - **4a**, **4b** and **6b** confirming their formulations. Perspective views of the corresponding molecular structures are shown in Figures 1 (**1a**), S1 (**2a**), S2 (**3a**), 2 (**4a**), 3 (**4b**) and 4 (**6b**), and selected bond lengths and angles are listed in Tables 2 (**1** − **4a**), 3 (**4b**) and 4 (**6b**).

The molecular structures of **1a** - **3a** can be visualized by assuming a distorted octahedral coordination around the Cd^{II} center, formed by two identical chelating bpy (**1a**), dmbpy (**2a**) or phen (**3a**) ligands and the dianionic *cis*-bis(phenylethynyl) platinate, which interacts with the cadmium center mainly through both C_α atoms and the Pt center. In the trpy derivatives (**4**), the cadmium center also adopts a distorted octahedral geometry, being bonded not only to the three nitrogen trpy atoms and the [Pt]($C\equiv CR)_2^{2-}$ unit (R = Ph **a**, Tol **b**), but also to an oxygen-donor solvent molecule, acetone in **4a** (Figure 2, d(Cd-O) = 2.461(3) Å) and acetone (Figure 3a, d(Cd-O) = 2.652(7) Å) or H_2O (Figure 3b, d(Cd-O) = 2.398(6) Å) in the case of **4b**. A search in the Cambridge database[66] did not come up with any complex containing acetone as a ligand towards Cd^{II} cation.

However, the observed Cd-O(acetone) distance in **4a** (2.461(3) Å) is similar to the Cd-O(OH$_2$) separation (2.398(6) Å) found in the second molecule of **4b**, and both of them are comparable to those reported for reference complexes containing other cetonic type molecules,[67-71] H$_2$O[49,72-75] or tetrahydrofurane[75] ligands. The longer Cd(1)-O(1)(acetone) separation (2.652(7) Å) found in **4b** indicates a weaker interaction. It is worthy to note that, in spite of the dicationic nature of the cadmium units and the known ability of [*cis*-Pt(C$_6$F$_5$)$_2$(C≡CR)$_2$]$^{2-}$ to act as an alkynylating agent,[76-78] no alkynylation process occurs in any case, although a σ- migration of one alkynyl group towards the Cd^{II} center unit should give a less polar doubly alkynyl σ/π type complex. However, this structural feature keeps the electron density on the platinum center and, presumably, allows it to form stronger Pt···Cd bonding interactions. In fact, the Pt-Cd separations ranging from 2.9998(3) Å in **4a** to 3.1163(4) Å in **2a** are comparable to those seen in the dianionic clusters [{Pt(μ-C≡CPh)$_4$}$_2$(CdCl)$_2$]$^{2-}$ **A** (Chart 1, 2.96 Å)[44] or [Pt$_9$(CO)$_{18}$(μ$_3$-CdCl$_2$)$_2$]$^{2-}$ (2.931(4) - 3.023(4) Å),[51] and clearly shorter than those observed in the η^2 alkynyl complexes **B** - **D** (Chart 1) (3.18 - 3.31 Å).[44,47] However, these distances are significantly longer than other unsupported Pt(II)-Cd(II) bonds such as those found in **E** (Chart 1, 2.764(1) Å)[46] or [Pt(Phpy)$_2$Cd(cyclen)]$^{+2}$ (2.639(1) Å)[48]. As mentioned above, the Cd^{II} is mainly interacting with the C$_\alpha$ carbon atoms of the C≡CR groups (μ-η^1 bonding) with Cd-C$_\alpha$ bond distances ranging from 2.355(7) to 2.554(5) Å, which are comparable to those seen in the [{*cis*-Pt(C$_6$F$_5$)$_2$(μ-C≡CPh)$_2$}Cd]$^{2-}$ dianion **D** (2.376(12)-2.418(10) Å).[47] The distances between the Cd^{II} center and the external C$_\beta$ carbon atoms are significantly longer (2.740(9)-2.949(7) Å), so they could be considered essentially non-bonding. We note that these distances are above the sum of the van der Waals radii (2.52 Å)[79] of carbon (1.43 Å) and the ionic radii of Cd^{II} (cn 6, 1.09 Å), and clearly

longer to that seen in previous asymmetrical η^2-alkynyl Cd derivatives, such as **C** (Chart 1, Cd-C_α, C_β 2.405(3), 2.556(4) Å).[47]

In all **1a-4a** and **4b** molecules the Cd center is displaced from the corresponding Pt(II) coordination planes (1.1519(2) Å **1a**; 1.3836(3) Å **2a**; 1.2261(4) Å **3a**; 1.3740(3) Å **4a**; 1.2479(5)-1.3255(5) Å **4b** Å), generating non planar V-shaped PtC$_4$Cd cores. The Cd-N distances fall in the range 2.317(6) to 2.412(4) Å, which are not unusual[74,75] for a six-coordinated environment at Cd.[79-83]

Furthermore, the molecular structure of **6b** (Figure 4a) differs from the isomer **1a** in the geometry of both metallic centers. Thus the Cd^{II} is bonded to four nitrogen atoms (2.327(7) - 2.405(7) Å) (see Table 4) of two bpy ligands and completes a five-coordination environment, being bonded to one of the mutually *trans* Pt-C_α bonds. The bonding interaction with the platinate unit can be compared to that seen in [*cis*-{Pt(C$_6$F$_5$)$_2$(C≡CPh)$_2$}Cd(cyclen)][46] (**E**, chart 1), but in **6b** the Pt-Cd vector exhibits a bigger displacement from the normal of the Pt coordination plane towards the alkynyl fragment (50.9(2)º). Thus, the Pt-Cd bond distance of 2.8966(6) Å (Table 4) is slightly shorter to that found in **1a** (3.1087(5), Table 2), but somewhat longer to that seen in the Pt-Cd cyclen derivative **E** (2.764(1) Å)[46] (chart 1). As a consequence, the Cd-Pt-C(1) angle (54.2(3)º) is more acute than that found in **E** (60.53º) and the Cd-C_α carbon length is significantly shorter (2.372(10) Å in **6b** *vs*. 2.493(4) Å in **E**). However, despite the fact the C(1)≡C(2)-Tol fragment is acting as μ-η^1-alkynyl bridging and the C(10)≡C(11)-Tol one as terminal, their structural parameters (angles at C_α and C_β and C≡C bond) are identical within experimental error (Table 4). The coordination of the Cd(bpy)$_2$ unit seems to slightly affect the Pt-C_α bonds (Pt-C(1) = 2.027(10) Å *vs*. Pt-C(10) = 1.981 (12) Å). It is now well established that in many heteropolynuclear Pt-M (M = Ag, Tl, Pb) pentafluorophenylplatinate complexes the presence of short *o*-F···M

contacts plays a key role contributing to the final stability of the complex.[84] In **6b** the dihedral angles formed by the pentafluorophenyl rings with the platinum coordination plane are 62.8 (3)° and 55.9(3)°; but the shortest Cd···*o*-F separation (Cd(1)···F(1) 3.485(7) Å) is longer than the sum of the van der Waals radii (3.05 Å),[79] showing that such contacts are not present here. Also, growing attention is being paid to the role that secondary interactions, such as π···π contacts and weak hydrogen bonds, play in determining the supramolecular self-assembly of small molecules to give three-dimensional networks,[85-89] and how the presence of these interactions can influence some physical properties such as solid-state photoluminescence, particularly in those systems involving square-planar d^8 complexes.[90-94] Further inspection of the crystal structures of the six complexes **1a** – **4a**, **4b** and **6b** reveals the presence of π···π contacts between aromatic ligands[85,90-92,95,96] (**1a**, **3a**, **4a**; distances between centroids of the aromatic rings 3.58 – 3.74 Å) and different types of weak intermolecular hydrogen bonds, [86] including C–H···π[91,94,97-101] (aromatic, C···C 3.29 – 3.77 Å, H···C 2.75 – 2.88 Å, C–H···C 170 – 114°; C≡C, C···C 3.50 – 3.79 Å, H···C 2.58-2.87 Å, C–H···C 170 – 132°), C–H···O[25,102,103] (C···O 3.25 – 3.56 Å, H···O 2.36 – 2.64 Å, C–H···O 171 – 123°) and C–H···F[85,104-107] (C···F 3.00 – 3.54 Å, H···F 2.32 – 2.89 Å, C–H···F 170 – 107°), leading to the generation of supramolecular 3-D networks. Although a more detailed description of all of these secondary interactions is shown in Figures S3 – S8 (see Supporting Information), Figure 4b shows, by way of an example, the *intra*- and *intermolecular* π···π contacts formed between one C_6F_5 ring (C(19) - C(24)) and a bpy ligand (N(1)-N(2)) of each molecule in complex **6b**, giving rise to an infinite mono-dimensional organization along the *c* axis (see also Figure S8 in Supporting Information). In the *intramolecular* contact, the distance from the centroid of the C_6F_5 ring to the plane formed by all the carbon and nitrogen atoms of the bpy ligand is 3.25

Å (minimum C···C and C···N distances of 3.45 and 3.15 Å, respectively) and the dihedral angle between the planes formed for both of the aromatic ligands is 5.6º; while in the *intermolecular* π···π contact the distance of the centroid of the C_6F_5 ring to the plane formed by the bpy ligand of the neighboring molecule is also 3.25 Å (minimum C···C and C···N distances of 3.36 and 3.68 Å, respectively) and the dihedral angle between the aromatic planes is 10.7º.

The most relevant features observed in the IR spectra of the *cis* derivatives **1 – 4** are the presence of two characteristic v$C\equiv C$ (2040 - 2075 cm^{-1}) and $v_{x\text{-sens}}$ C_6F_5 (780 – 800 cm^{-1}) bands, confirming the retention of the *cis-* geometry of the platinate entities. In the diimine derivatives (**1-3**), the expected shift to lower wavelengths of the v$C\equiv C$ bands (2075 - 2060 cm^{-1}) relative to the precursors (PMePh$_3$)$_2$[*cis*-Pt(C_6F_5)$_2$($C\equiv CR$)$_2$] (R = Ph 2096, 2083 cm^{-1}; R = Tol 2091, 2078 cm^{-1}) is lesser than that observed in the trpy complexes (**4a** 2060, 2044 cm^{-1}; **4b** 2054, 2040 cm^{-1}), suggesting that the interaction of the Cd centers of the Cd(N-N)$_2^{+2}$ units with the alkynyl ligands is presumably weaker. With regard to the *trans* complexes **6**, it is worth noting that their IR spectra confirm not only the presence of terminal and bridging alkynyl ligands, but also the formation of the donor-acceptor Pt(II)→Cd(II) bond. Thus, they show one medium v$C\equiv C$ band (2068 cm^{-1}) slightly shifted to lower wavenumbers when compared with the precursors [*trans*-Pt(C_6F_5)$_2$($C\equiv CR$)$_2$]$^{2-}$ (R = Ph **5a** 2077 cm^{-1};[59] R = Tol **5b** 2079 cm^{-1}), which is attributed to the μ-$\eta^1 C\equiv CR$ bridging group. Interestingly, in both complexes the strong v$C\equiv C$ band due to the terminal alkynyl ligand appears notably shifted to higher frequencies (2104 **6a**; 2108 cm^{-1} **6b**). This fact is consistent with the formation of the Pt→Cd bond, which decreases the electron density at the Pt(II) center and, as a consequence, its donor capability towards the π^* orbitals of the $C\equiv CR$ groups. We have previously observed similar behavior in some alkynyl-based Pt-Tl complexes that have Pt-Tl bonds.[27,29]

Conductivity measurements of **1b** – **4b** and **6b** derivatives (see experimental) are consistent with the integrity of the bimetallic complexes in solution. However, fluxional behavior is evident by ^{1}H and ^{19}F NMR spectroscopy (CD$_3$COCD$_3$). Thus, the ^{1}H and ^{19}F NMR of the *cis* derivatives **1** - **4** are very simple, revealing the presence of only one set of alkynyl, chelating (diimine **1-3**, trpy **4**), and C$_6$F$_5$ groups. The proton spectra indicate that both halves of the chelating ligands are equivalent and the ^{19}F NMR spectra display typical AA´MM´X systems (2 *o*-F, *p*-F, 2 *m*-F), also indicating effective equivalence of the *o*-F atoms, as well as the *m*-F atoms. Similar spectra were found for representative complexes **1b** and **4b** at low temperature (see experimental). The observed spectra could be explained by assuming a very fast inversion of the central bent (V-shape) dimetallacycle [Pt](C≡CR)$_2$[Cd], without excluding a possible simultaneous free rotation of the C$_6$F$_5$ rings around the Pt-C$_{ipso}$ bonds. This behavior has been previously observed in many bi- and trinuclear complexes stabilized by either strongly bent chelating type (V shape) or slightly bent (σ,π type) double alkynyl bridging systems [M](μ-C≡CR)$_2$[M´].[76,106,108] The ^{13}C{^{1}H}NMR spectrum of **4b** displays the expected signals for the trpy ligand and one set of C≡CTol groups. In accordance with previous observations,[47] the C$_\alpha$ and C$_\beta$ carbon atoms are significantly up and downfield shifted, respectively, in relation to the precursor (δC$_\alpha$/C$_\beta$ 90.4/113.3 in **4b** *vs* 117.3/103.7 in [*cis*-Pt(C$_6$F$_5$)$_2$(C≡CTol)$_2$]$^{2-}$), a feature which also confirms that the interaction of the alkynyl ligand with the Cd^{II} center is present in solution. For the *trans* derivatives **6**, their scarce solubility precluded their characterization by ^{13}C{^{1}H} NMR spectroscopy. Again, the ^{1}H and ^{19}F NMR spectra in CD$_3$COCD$_3$ at room temperature are very simple, revealing only one set of bpy, alkynyl and C$_6$F$_5$ rings (see experimental). By decreasing the temperature to 173 K, similar AB (Tol) and AA´MM´X (2*o*-F; 2*m*-F; *p*-F) spin systems were observed for aromatic protons and

fluorine of C_6F_5 groups for the tolylethynylderivative **6b**. Moreover, the addition at this low temperature of a small amount of the precursor $(NBu_4)_2[trans-Pt(C_6F_5)_2(C\equiv CTol)_2]$ **5b** gives rise to ^{1}H and ^{19}F NMR spectra containing separate signals of **6b** and **5b**, thus suggesting that fast dissociation of the "$Cd(bpy)_2^{2+}$" unit is not responsible for the apparent D_2h symmetry. The observed spectra are presumably caused by a fast exchange of the "$Cd(bpy)_2^{2+}$" unit between both alkynyl groups with simultaneous migration above and below the platinum coordination plane. Nevertheless, simple free rotation of C_6F_5 groups with the simultaneous fast alkynyl exchange of the cadmium unit is also likely.

Optical Properties

The electronic spectra of the tolylethynyl binuclear derivatives **1b** - **6b** were recorded in CH_2Cl_2 (Table 5) and 2-MeTHF (Table S1), without any significant modification with the solvent change, except for a better vibronic resolution on CH_2Cl_2 spectra. The related phenylethynyl complexes **1a** – **4a**, **6a** are rather insoluble, so their UV-Vis spectra could not be performed. The CH_2Cl_2 5 x 10^{-5} M UV-Vis spectra of **1b** – **6b** show high energy absorptions (220-295 nm) and low energy bands at ca. 303-336 nm. The former are assigned as intraligand transitions ($\pi\pi^*$) of anionic (C_6F_5, $C\equiv CTol$) and neutral diimine (**1b** - **3b**, **6b**) or trpy ligands (**4b**). As can be observed in Figure 5 for complexes **1b-3b**, the more intense low energy absorptions follow the order 292 nm **3b** (phen) > 307 **1b** (bpy) >303, 315*sh* **2b** (dmbpy), although complex **3b** also exhibits a low energy shoulder at 311 nm. The fact that the lowest energy absorption appears in the bimetallic complex having the "$Cd(dmbpy)_2$" unit, with the higher π^*(N-N) orbital, suggests that the diimine ligands are not likely to be the target orbital. In the three complexes, this low energy absorption is blue shifted in relation to the mixed ^{1}IL/^{1}MLCT ($C\equiv CTol$) band in the bis(alkynyl)platinate precursor $(PMePh_3)_2[cis-$

Pt(C$_6$F$_5$)$_2$(C≡CTol)$_2$] (311, 334sh nm). It seems likely that the interaction of the Platinum and both C$_\alpha$ alkynyl atoms with the Cd(N-N)$_2$$^{+2}$ unit causes a stabilization of the Pt/C≡C based HOMO. Under this assumption and the fact that ππ* intraligand transition of the diimine ligands also occurs at similar energies, the lower energy features are assigned as admixtures of MLCT (d(Pt)→π*C≡CTol) and intraligand IL (C≡CTol, diimine) transitions. The trpy derivative **4b** exhibits a more complex profile in this region, with three peaks (at ca. 307, 321, 334 nm), in agreement with a remarkable contribution of the low-lying trpy localized IL state, also likely with some admixture of alkynyl (ππ* C≡CTol) and MLCT(Pt→alkynyl) charge transfer.

Based on our previous works[26,27,46,47,109] and other related recent studies[110,111] on alkynyl platinum complexes, the lowest energy absorption (334, 342sh **5a**; 331, 338sh **5b**) in the mononuclear complexes (NBu$_4$)$_2$[$trans$-Pt(C$_6$F$_5$)$_2$(C≡CR)$_2$] **5** (R = Ph **a**, Tol **b**) is attributed to an admixture of ππ*(C≡CR) ^{1}IL/dπ(Pt)→π*(C≡CR) MLCT, with a predominant intraligand character. In both complexes, this band is red shifted compared to the corresponding cis- isomers Q$_2$[cis-Pt(C$_6$F$_5$)$_2$(C≡CR)$_2$] (R = Ph 310, 325 nm; R = Tol 311, 331 nm)[47] in agreement with previous observations in related cis- and $trans$-configured bis(alkynyl)bis(phosphines)platinum complexes, confirming that the extent of π delocalization through the Pt is more efficient when the alkynyl groups are mutually $trans$.[112] We have also observed that the intensity of this low energy ^{1}MLCT/^{1}IL(C≡CR) band is remarkably higher in the $trans$ derivatives than in the related cis ones (i.e. 338 nm, ε = 30.0 x 10^3 M^{-1}cm^{-1} in **5b** vs 331 nm, 7.2 x 10^3 M^{-1}cm^{-1} in (PMePh$_3$)$_2$[cis-Pt(C$_6$F$_5$)$_2$(C≡CTol)$_2$]^{47}) illustrating again the good electronic communication of the ethynyl fragments in the former, and the stronger CT character (more allowed) of the transition in the $trans$ geometry. As can be seen in Figure 6 the most remarkable difference of the UV spectra of complex **6b**, built from **5b** and

"Cd(bpy)$_2$$^{+2}$", in comparison to its precursor **5b** is the weaker intensity of the ^{1}MLCT/^{1}IL transition (336 nm, ε = 12.3 x 10^3 M^{-1}cm^{-1} **6b** *vs* 338 nm, ε = 30.0 x 10^3 M^{-1}cm^{-1} **5b**), thus suggesting that the formation of the Pt-Cd bond probably hinders communication between the tolylethynyl fragments. The small hipsochromic shift (2 nm) is in accordance with the expected decrease of the electron density on the platinum center upon formation of the Pt-Cd bond, which increases the energy of the ^{1}MLCT component. However, the band is broader than in **5b** and exhibits a long tail extending to the visible, in agreement with its yellow color.

All complexes (except **6**) display luminescence in solid state and for the tolyl ethynyl derivatives emission is also observed in 2-MeTHF both at 298 (weak) and at 77 K. The photophysical data are summarized in Tables 6 (solid) and S2 (solution, glass), and illustrative examples are shown in Figures 7 and 8 (**1b-4b**), S9 (**1a-4a**), 9 (**5b**) and 10 (**6b**).

As can be observed in Figure 7, in solid state at room temperature the tolylalkynyl complexes **1b-3b** exhibit a similar low energy green emission (λ$_{max}$ 495 **1b**, **2b**; ~505 nm **3b**), clearly structured in **1b** and **2b**, together with a very weak emission on the high energy side (~ 450 **1b**, **2b**; 440 - 473 nm **3b**). The lifetime of the low energy band fits to a monoexponential decay in the range of microseconds (32 μs **1b**; 43 μs **2b**; 14 μs **3b**), indicative of triplet parentage. At 77 K, the contribution of the high energy component increases in **1b** and **2b**, while complex **3b** mainly shows the low energy emission as a better structured band (492, 521 nm). The apparent vibronic structure observed in the lower energy band, either at room (827 - 934 cm^{-1}) or low temperature (1131 - 1606 cm^{-1}), and the extremely long lifetimes (i.e. 120 μs for **3b**) are suggestive of emission coming from ^{3}ππ* intraligand centered states. Although, the influence of the diimine groups in the maxima is minimal (see Table 6), this lower energy band is ascribed to

metal-perturbed (Pt, Cd) $\pi\pi^*$ alkynyl (C≡CTol) phosphorescence, likely mixed with some $\pi\pi^*$(diimine) character. The high energy emission, that is observed at ca. 450 nm (77 K) for **1b** and **2b**, resembles that seen in the precursor (PMePh$_3$)$_2$[cis-Pt(C$_6$F$_5$)$_2$(C≡CTol)$_2$] at low temperature (451$_{max}$, λ_{ex} 360 nm),[47] being thus assigned to a ^{3}IL $\pi\rightarrow\pi^*$ (C≡CTol) manifold. It is worth noting that for complex **1b** the emission profile at 77 K exhibits two peaks at 453 nm and 483 nm, but whereas the decay monitoring at 450 nm fits to one component (81 μs), the band at 483 nm fits to two components with different lifetimes (152 μs 14%; 68 μs 86%), in agreement with the presence of two emissive states or weakly coupled relaxation channels. In contrast to this behavior, complex **4b** containing the "Cd(trpy)" unit shows, at room temperature, a broad featureless peak at 527 nm with a monoexponential decay lifetime of 12 μs, which is slightly blue-shifted at 77 K (517 nm). This blue shift is most likely to be caused by increased environment rigidity, which is consistent with the reduced thermal vibrational relaxation.[113,114] In this complex, band shape lacks the typical structure associated with those ligand-centered transitions, pointing to a more metal (Pt, Cd) character associated with the transition. Moreover, at 77 K the emission phosphorescence fits well to a biexponential decay, having a major component (88%) of 50 μs and a minor one (12%) in the milliseconds range (1.1 ms), suggesting that it also has ligand contribution. Thus, this emission could be tentatively attributed to the coupling of metal-metal (Pt-Cd) charge transfer (MM′CT) and intraligand (trpy, C≡CTol) transitions.

In the related phenylethynyl derivatives **1a-4a**, the influence of the chelating diimine ligand is more apparent. As can be observed in Figure S9, the terpyrydyne bimetallic complex **4a** exhibits a structured emission at 298 K (493, 520 nm) which becomes well resolved at 77 K (460sh, 485$_{max}$, 523, 560sh nm). Both, the weak shoulders at 460 nm

and the dual exponential decay monitored at the λ_{max} (485 nm) with two long lifetime components of 30.2 (55%) and 0.6 (45%) milliseconds, suggest the contribution of close emissive states. The vibronic spacing of the more intense emission at 77 K (1499, 1263 cm^{-1}) is in agreement with the implication of the trpy ligand in the emission. Structured profiles (443 - 523 nm) with dual exponential decays in the millisecond range (0.3 - 30.2 ms) are also seen for **1a-3a** at low temperature (77 K) (see Figure S9). Hence, we conclude that these emissions are most likely originated from metal (Pt, Cd) perturbed spin-forbidden ligand centered states, involving the coligands in the cationic cadmium unit (trpy **4a**, N-N **1a-3a**) and the C≡CPh groups. No clear correlation can be made when comparing the emission of both series (**a** *vs* **b**) or when comparing the nitrogen donor coligands in each series.

For **1b-4b**, the emission spectra have been recorded in solution (2-MeTHF, 77 K, 298 K, Table S2). In frozen 2-MeTHF glasses, all complexes exhibit clear structured bands with vibronic spacing (~ 1450 - 1590; 990 - 1271; 1083 - 1222 cm^{-1}), which are characteristic of the C-N and C-C stretching motion of the chelating N-heterocycle frameworks. As can be observed in Figure 8, the emission maxima (433 **1b**, 445 **2b**, 451 **3b** and 438 nm **4b**) correlate well with those seen in the N-containing free ligands (~ 370, λ_{ex} = 330 bpy; 394, λ_{ex} = 340 dmbpy; 400, 420, λ_{ex} = 370 phen; 441, λ_{ex} = 384 nm trpy). This similarity allows us to assign the emission to intraligand (diimine **1b-3b**, trpy **4b**) $^3\pi\pi^*$ phosphorescence though, the presence of multicomponents in the lifetime decays (see Table S2) suggests that other states could also contribute somehow to the emission. Due to the electron donating properties of the platina-bis(alkyne) unit and the acceptor character of the polyimine groups, some mixing with a ligand(alkyne) to ligand(imine) charge transfer (^{3}LL′CT) mediated through the metallic (Cd or Pt, Cd) core can not be excluded. Weaker, but also structured (1402-1103 cm^{-1}), emission

profiles are observed in fluid (298 K) solution. The emission onsets are blue shifted in compared to those observed in glassy solutions, and occur at very similar energies (~ 402, ~ 425, ~ 450 nm) in all **1b-4b** complexes, probably due to their broader appearances. Only the trpy derivative **4b** exhibits an additional (less intense) low energy peak centered at 492 nm, probably coming from an emissive state related to the Pt···Cd bonding interaction. Although too weak for lifetime measurements, the high energy band in all derivatives is tentatively assigned to ^{3}IL(polyimine), since it is related to a similar low energy excitation feature located at 360 nm well above the ^{1}IL absorption maxima (see Table S2).

As many bis(alkynyl)platinum complexes, *trans* configured anionic precursors **5a** and **5b** also exhibit luminescence in solid state, both at room and low temperature (77 K). The emissions show the expected structured bands (see Table 6) with progressive spacing modes indicative of the combination of C≡C and aryl rings, which, on the basis of previous assignments, is attributed to phosphorescence coming from mixed ^{3}IL/^{3}MLCT ($\pi \rightarrow \pi^*$(C≡CR)/dπ(Pt)/C≡CR) manifold. In the tolylethynyl derivative **5b** the emission maxima is slightly red shifted in relation to **5a** (460 **5b** *vs* 457 nm **5a** at 77 K), and in both complexes a slight red-shift in energy is observed when comparing with the corresponding $Q_2[cis\text{-}Pt(C_6F_5)_2(C≡CR)_2]$ (R = Ph 444 nm, R = Tol 451 nm, 77 K).[47] This feature is consistent with previous theoretical calculations[115] carried out on bis(acetylide) neutral complexes, which indicate that the mixing of dπ (and p) orbitals of the Pt center with the π and π^* MOs of the alkynyl groups leads to π-type conjugation through the metal center, this delocalization being favored in the *trans* isomers.[116] The emission has also been examined in solution (Table S2). At 298 K, a very weak high energy structured emission is detected (λ_{max} 400 **5a**, 402 nm **5b)** in 2-MeTHF tentatively ascribed as ^{1}IL fluorescence. Upon freezing at 77 K, well resolved site-

selectivity dual structured emissions are observed, both in CH_2Cl_2 and 2-MeTHF glasses. As is seen in Figure 9 for **5b**, in CH_2Cl_2 5 x 10^{-4} M glass excitation at 350 nm gives rise to a low energy emission with λ_{max} at 452 nm, whereas excitation at shorter wavelengths (λ_{max} 320 nm) produces a similar structured profile but shifted to higher energies (λ_{max} 437 nm). As it is also observed, the corresponding excitation spectra differ mainly on the low energy red-side, suggesting the presence of sample heterogeneity in the glass or two close emissive states. The observation of dual site-selectivity emissions in alkynyl platinum complexes is not unprecedented.[47,117-119] In particular, splitting in the phosphorescence at low temperature has been attributed to the existence of different conformers (planar or twisted), that can not equilibrate in the frozen matrix.[117-119] We recently observed a similar photoselection in the trimetallic complex $(NBu_4)_2[\{cis\text{-}Pt(C_6F_5)_2(\mu\text{-}C{\equiv}CPh)_2\}_2Cd]$ (**D**, chart 1)[47], and it was tentatively ascribed to the presence of two distinct $^3\pi\pi^*$ and ^{3}MLCT (or mixed $^3\pi\pi/^3$MLCT) excited states that are not coupled. Due to the difference in the excitation spectra (Figure 9), a similar explanation could be operative in complexes **5**, but the simultaneous existence of different conformers seems more likely.

Complex **6a** and **6b** are essentially non emissive in solid state at 298 K. Upon cooling (77 K), **6a** shows a structured emission (478, 495 nm), while **6b** displays two luminescence bands (455 and 520 nm, see Figure 10) regardless of the λ_{ex} used (350 - 400 nm). For this latter (**6b**), lifetime measurements (see Table 6) and excitation spectra in both maxima suggest that each emission derives from a different excited state. In frozen solution (Table S2), complex **6b** only exhibits a slightly structured high energy emission (445, 482 nm CH_2Cl_2; 449, 492 nm 2-MeTHF), suggesting that the low unstructured energy emission centered at 520 nm seen in solid state at 77 K is likely to be due to $\pi{\cdots}\pi$ stacking interactions. In support of this assignment, such *intra-* and

intermolecular π···π interactions were observed in the extended lattice of **6b** in solid state (see Figure 4b). The resemblance of the high energy emissions with those seen in the precursors **5** is suggestive of an emission coming from the platinate unit "[*trans*-Pt(C$_6$F$_5$)$_2$(C≡CR)$_2$]" (^{3}IL/^{3}MLCT manifold) perturbed by the short donor acceptor Pt→Cd bond. The small hipsochromic shift seen for **6a** (448 nm) and **6b** (455 nm) in solid state at 77 K in relation to the precursors **5a** (457 nm) and **5b** (460 nm), respectively, could probably be attributed to the stabilization of the energy of the Pt(d)/πC≡CR based HOMO due to the formation of the Pt→Cd donor-acceptor bond.

Conclusions.

In summary, the utilization of anionic *cis*- or *trans*-[Pt(C$_6$F$_5$)$_2$(C≡CR)$_2$]$^{2-}$ (R = Ph, Tol) as building blocks for the *in situ* generated "Cd(N-N)$_2$$^{2+}$" and "Cd(trpy)$^{2+}$" units successfully gives heterobimetallic Pt-Cd complexes **1 - 4** and **6**. It is interesting to note that while the *cis*- precursors connect the "Cd(N-N)$_2$$^{2+}$" units through both Pt-C$_\alpha$ bonds, completing distorted pseudo-octahedral environments around the Cd center in complexes [*cis*-Pt(C$_6$F$_5$)$_2$(C≡CR)$_2$Cd(N-N)$_2$] **1 - 3**, the *trans*- isomers employ only one of the Pt-C$_\alpha$ bonds, giving rise to a distorted trigonal-bypyramidal coordination in [*trans*-Pt(C$_6$F$_5$)$_2$(C≡CR)$_2$Cd(bpy)$_2$] (**6**). As a consequence, both the Pt-Cd and Cd-C$_\alpha$ bond distances are remarkably shorter in **6b** in relation to **1a – 3a**. The cadmium center of the dicationic "Cd(trpy)$^{2+}$" unit in [*cis*-Pt(C$_6$F$_5$)$_2$(C≡CR)$_2$Cd(trpy)] **4a** and **4b** has a similar distorted octahedral environment to those of **1 – 3**, being also bonded to both Pt-C$_\alpha$ of the [Pt](C≡CR)$_2$$^{2-}$ unit and contacting weakly with a solvent molecule (acetone **4a**; acetone/H$_2$O **4b**). In solid state, bimetallic complexes **1 – 4**, having *cis*-configured platinum fragments, show blue and/or green phosphorescence with contribution of states of different nature. For the tolylderivatives **1b – 3b**, the high energy structured emissions (blue region) were assigned to a ^{3}IL π→π*(C≡CTol) manifold, while the

lower energy features (green region) to metal (Pt-Cd) perturbed alkynyl C≡CTol phosphorescence, likely mixed with some diimine character. Complex **4b**, having shorter Pt-Cd bond, exhibits a green emission (527 nm, 298 K, monoexponential decay; 517 nm, 77 K, biexponential decay) tentatively attributed to the coupling of metal-metal (Pt-Cd) charge transfer (MM'CT) and intraligand (trpy, C≡CTol) transitions. In glassy state (2-MeTHF) complexes **1b** − **4b** exhibit structured emissions mainly ascribed to (diimine **1b** − **3b**; trpy **4b**)$^3\pi\pi^*$ phosphorescence, probably mixed with some ligand (alkyne) to ligand (polyimine) charge transfer ^{3}LL'CT. In the related phenylethynyl derivatives **1a** − **4a**, the influence of the polyimine is more apparent, exhibiting structured profiles with dual exponential decays in the millisecond range, which are likely to originate from metal (Pt, Cd) perturbed spin forbidden ligand-centered states (poliimine and C≡CPh groups). In complexes [*trans*-Pt(C$_6$F$_5$)$_2$(C≡CR)$_2$Cd(bpy)$_2$] **6**, the formation of the very short Pt–Cd bonds (2.8966(6) Å, **6b**) quenches the blue emission (^{3}IL(C≡CR)/^{3}MLCT manifold) of the precursors (NBu$_4$)$_2$[*trans*-Pt(C$_6$F$_5$)$_2$(C≡CR)$_2$] **5** in solid state at room temperature. At 77 K, these bimetallic derivatives display a high structured band assigned to the mixed ^{3}IL/MLCT (L = C≡CR) manifold perturbed by the donor-acceptor Pt→Cd bond and, in the case of **6b**, an additional low energy feature (which is absent in 2-MeTHF solution fluid and glass), tentatively ascribed to $\pi\pi$ stacking interactions.

Supporting Information Available: Complete details concerning the synthesis and spectroscopic characterization of the complexes **1** − **6**. Data for the electronic spectra of **1b** - **6b** and **5a** recorded in 2-MeTHF (Table S1). Data for the emission spectra and lifetimes measurements of complexes **1** − **6** in solution at 298 and 77 K (Table S2).

ORTEP view of the complexes **2a** and **3a** (Figure S1 and S2). Figures of the tridimensional organization of complexes **1a**, **2a**, **3a**, **4a**, **4b** and **6b** (Figures S3 – S8). Emission spectra of crystalline samples of **1a**, **2a**, **3a** and **4a** at 298 and 77 K (Figure S9). Crystallographic data in CIF format. This material is available free of charge via the Internet at http://pubs.acs.org.

Footnotes

* Corresponding authors. E-mail: elena.lalinde@unirioja.es (E. L.).

jesus.berenguer@unirioja.es (J. R. B.)

† Universidad de La Rioja, UA-CSIC

‡ Universidad de Zaragoza-CSIC

References

(1)   Chou, P. T.; Chi, Y. *Chem. Eur. J* **2007**, *13*, 380.

(2)   Cooke, M. W.; Hanan, G. S. *Chem. Soc. Rev* **2007**, *36*, 1466.

(3)   Evans, R. C.; Douglas, P.; Winscom, C. J. *Coord. Chem Rev* **2006**, *250*, 2093.

(4)   Holder, E.; Langeveld, B. M. W.; Schubert, U. S. *Adv. Mater.* **2005**, *17*, 1109.

(5)   McClenaghan, N. D.; Leydet, Y.; Maubert, B.; Indelli, M. T.; Campagna, S. *Coord. Chem Rev* **2005**, *249*, 1336.

(6)   Kato, M. *Chem. Soc. Jpn.* **2007**, *80*, 287 and references therein.

(7)   Yam, V. W.-W.; Cheng, E. C. C. *Top Curr. Chem.* **2007**, *281*, 269.

(8)   Fernandez, E. J.; Laguna, A.; Lopez de Luzuriaga, J. M. *Dalton Trans.* **2007**, 1969.

(9)   Hang, M.; Huynh, V.; Dattelbaum, D. M.; Meyer, T. J. *Coord. Chem Rev* **2005**, *249*, 457.

(10)   Thanasekaran, P.; Liao, R. T.; Liu, Y. H.; Rajendran, T.; Rajagopal, S.; Lu, K. L. *Coord. Chem Rev* **2005**, *249*, 1085.

(11)   de Bettencourt-Dias, A. *Dalton Trans.* **2007**, 2229.

(12)   Yam, V. W.-W.; Cheng, E. C. C. *Top Curr. Chem.* **2005**, *257*, 1.

(13)   Puddehphatt, R. J. *Chem. Commum.* **1998**, 1055.

(14)   Williams, J. A. G. *Top Curr. Chem.* **2007**, *281*, 205.

(15)   Chen, Z. N.; Zhao, N.; Fan, Y.; Ni, J. *Coord. Chem Rev* **2009**, *253*, 1.

(16)   Silverman, E. E.; Cardolaccia, T.; Zhao, X.; Kim, K. Y.; Haskins-Glusac, K.; Schanze, K. S. *Coord. Chem. Rev.* **2005**, *249*, 1491.

(17)   Wong, K. M. C.; Yam, V. W.-W. *Coord. Chem Rev* **2007**, *251*, 2477.

(18)   Castellano, F. N.; Pomestchenko, I. E.; Shikhova, E.; Hua, F.; Muro, M. L.; Rajapakse, N. *Coord. Chem. Rev.* **2006**, *250*, 1819.

(19)   Hissler, M.; McGarrah, J. E.; Connick, W. B.; Geiger, D. K.; Cummings, S. D.; Eisenberg, R. *Coord. Chem. Rev.* **2000**, *208*, 115.

(20)   Ziessel, R.; Hissler, M.; El-ghayoury, A.; Harriman, A. *Coord. Chem. Rev.* **1998**, *178 -180*, 1251.

(21)   Wong, W. Y. *Dalton Trans.* **2007**, 4495 and references therein.

(22)   Lagunas, M. C.; Fierro, C. M.; Pintado-Alba, A.; de la Riva, H.; Betanzos-Lara, S. *Gold Bull.* **2007**, *40*, 135.

(23)   Chen, Z. N.; Fan, Y.; Ni, J. *Dalton Trans.* **2008**, 573 and references therein.

(24)   Ziessel, R.; Seneclavze, J. B.; Ventura, B.; Barbieri, A.; Barigelletti, F. *Dalton Trans.* **2008**, 1686 and references therein.

(25)   Gil, B.; Forniés, J.; Gómez, J.; Lalinde, E.; Martin, A.; Moreno, M. T. *Inorg. Chem.* **2006**, *44*, 7788.

(26)   Forniés, J.; Fuertes, S.; Martín, A.; Sicilia, V.; Lalinde, E.; Moreno, M. T. *Chem. Eur. J* **2006**, *12*, 8253.

(27)   Berenguer, J. R.; Forniés, J.; Gil, B.; Lalinde, E. *Chem. Eur. J.* **2006**, *12*, 785.

(28)   Ara, I.; Berenguer, J. R.; Eguizabal, E.; Forniés, J.; Gómez, J.; Lalinde, E. *J. Organomet. Chem.* **2003**, *670*, 221.

(29)   Charmant, J. P. H.; Forniés, J.; Gómez, J.; Lalinde, E.; Merino, R. I.; Moreno, M. T.; Orpen, A. G. *Organometallics* **2003**, *22*, 652.

(30)   Charmant, J. P. H.; Forniés, J.; Gómez, J.; Lalinde, E.; Merino, R. I.; Moreno, M. T.; Orpen, A. G. *Organometallics* **1999**, *18*, 3353.

(31)   Wong, W. Y. *Coord. Chem Rev* **2007**, *251*, 1739.

(32)   Chui, S. S. Y.; Ng, M. F. Y.; Che, C. M. *Chem. Eur. J.* **2005**, *11*, 1739.

(33)   Yam, V. W.-W.; Lo, K. K.-W.; Wong, K. M.-C. *J. Organomet. Chem.* **1999**, *578*, 3.

(34)   Yam, V. W.-W.; Lo, K. K. W.; Fung, W. K. M.; Wang, C. R. *Coord. Chem Rev* **1998**, *171*, 17.

(35)   Ferrer, M.; Mounir, M.; Rodriguez, L.; Rossell, O.; Coco, S.; Gomez-Sol, P.; Martin, A. *J. Organomet. Chem.* **2005**, *690*, 2200.

(36)   Lin, Y. Y.; Lai, S. W.; Che, C. M.; Cheung, K. K.; Zhou, Z. Y. *Organometallics* **2002**, *21*, 2275.

(37)   Chao, H. Y.; Lu, W.; Li, Y.; Chan, M. C. W.; Che, C. M.; Cheung, K. K.; Zhu, N. *J. Am. Chem. Soc.* **2002**, *124*, 14696.

(38)   Higgs, T. C.; Parsons, S.; Bailey, P. J.; Jones, A. C.; MacLachlan, F.; Parkin, A.; Dawson, A.; Tasker, P. A. *Organometallics* **2002**, *21*, 5692.

(39)   Liao, Y.; Feng, J. K.; Yang, L.; Reu, A. M.; Zhang, H. X. *Organometallics* **2005**, *24*, 385.

(40)   Nast, R.; Richers, L. *Z. Anorg. Allg. Chem.* **1963**, *319*, 320.

(41)   Jeffery, E. A.; Mole, T. *J. Organomet. Chem.* **1968**, *11*, 393.

(42)   Barr, D.; Edwards, A. J.; Raithby, P. R.; Rennie, M. A.; Verhorevoort, K.; Wrich, D. S. *J. Chem. Soc., Chem. Commun.* **1994**, 1627.

(43)   Harms, K.; Merle, J.; Maichle-Mössmer, C.; Massa, W.; Krieger, M. *Inorg. Chem.* **1998**, *37*, 1099.

(44)   Charmant, J. P. H.; Falvello, L. R.; Forniés, J.; Gómez, J.; Lalinde, E.; Moreno, M. T.; Orpen, A. G.; Rueda, A. *Chem. Commun.* **1999**, 2045.

(45)   Forniés, J.; Gómez, J.; Lalinde, E.; Moreno, M. T. *Inorg. Chem.* **2001**, *40*, 5415.

(46)   Forniés, J.; Ibañez, S.; Martín, A.; Gil, B.; Lalinde, E.; Moreno, M. T. *Organometallics* **2004**, *23*, 3963.

(47)   Fernández, J.; Forniés, J.; Gil, B.; Gómez, J.; Lalinde, E.; Moreno, M. T. *Organometallics* **2006**, *25*, 2274.

(48)   Yamaguchi, T.; Yamazaki, F.; Ito, T. *J. Am. Chem. Soc.* **1999**, *121*, 7405.

(49)   Li, Z.; Zheng, W.; Liu, H.; Mok, K. F.; Hor, T. S. A. *Inorg. Chem.* **2003**, *42*, 8481.

(50)   Chen, W.; Liu, F.; Nishioka, T.; Matsumoto, K. *Eur. J. Inorg. Chem.* **2003**, 4234.

(51)   Femoni, C.; Kaswalders, F.; Iapalucci, M. C.; Longoni, G.; Zachini, S. *Chem. Commum.* **2006**, 2135.

(52)   Balzani, V.; Saudola, F. *Supramolecular Photochemistry*; Wiley: Chichester, 1993.

(53)   Kalynasundaran, K. *Photochemistry of Polypiridine and Polyphyrin Complexes*; Academic Press.: London, 1992.

(54)   Horvath, O.; Stevenson, K. L. *Photochemistry of Coordination Compounds*; VCH: New York, 1993.

(55)   Lehn, J. M. *Supramolecular Chemistry: Concepts and Perspectives*; VCH: Weinheim, 1995.

(56)   Chen, W. T.; Wang, M. S.; Liu, X.; Guo, G. C.; Hvang, J. S. *Cryst. Growth. Des.* **2006**, *6*, 2289 and references therein.

(57)   Shi, X.; Zhu, G.; Wang, X.; Li, G.; Fang, Q.; Zhao, X.; Wu, G.; Tian, G.; Xue, M.; Wang, R.; Qiu, S. *Cryst. Growth Des.* **2005**, *5*, 341.

(58)   Espinet, P.; Forniés, J.; Martínez, F.; Sotés, M.; Lalinde, E.; Moreno, M. T.; Ruíz, A.; Welch, A. J. *J. Organomet. Chem.* **1991**, *403*, 253.

(59)   Ara, I.; Berenguer, J. R.; Forniés, J.; Lalinde, E.; Moreno, M. T. *Organometallics* **1996**, *15*, 1820.

(60)   Otwinowski, Z.; Minor, W. *Methods in Enzymology* **1997**, *276*, 307 - 326.

(61)   Sheldrick, G. M. *SHELX-97, a program for the refinement of crystal structures* University of Göttingen, Germany, 1997.

(62)   Beursken, P. T.; Beursken, G.; Bosman, W. P.; de Gelser, R.; García-Granda, S.; Gould, R. O.; Smith, J. M. M.; Smykalla, C. *The DIRDIF92 program system*; Technical Report of the Crystallography Laboratory: University of Nijmegen: The Netherlands, 1992.

(63)   Blessing, R. H. *Acta Crystallogr.* **1995**, *A51*, 33.

(64)   Parkin, S.; Moezzi, B.; Hope, H. *J. Appl. Cryst.* **1995**, *28*, 53.

(65)   Forniés, J.; García, A.; Lalinde, E.; Moreno, M. T. *Inorg. Chem.* **2008**, *47*, 3651.

(66)   Search performed with *The Cambridge Structural Database 5.30* (November 2008); The Cambridge Crystallographic Data Centre, 2008.

(67)   Chen, X.-D.; Mak, T. C. W. *Inorg. Chem. Commun.* **2005**, *8*, 393.

(68)   Goher, M. A. S.; Mautner, F. A.; Abu-Youssef, M. A. M. *J. Chem. Soc., Dalton Trans.* **2002**, 3309.

(69)   Danil de Namor, A. F.; Chahine, S.; Kowalska, D.; Castellano, E. E.; Piro, E. E. *J. Am. Chem Soc.* **2002**, *124*, 12824.

(70)   Casas, J. S.; Castellano, E. E.; García-Tasende, M. S.; Sánchez, A.; Sordo, J.; Zukerman-Schpector, J. *Z. Anorg. Allg. Chem.* **1997**, *623*, 825.

(71)   Balegroune, F.; Braunstein, P.; Douce, L.; Dusausoy, Y.; Grandjean, D.; Knorr, M.; Strampfer, M. *J. Cluster Sci.* **1992**, *3*, 275.

(72)   Bazzicalupi, C.; Bencini, A.; Bianchi, A.; Borsari, L.; Danesi, A.; Giorgi, C.; Mariani, P.; Pina, F.; Santarelli, S.; Valtancoli, B. *Dalton Trans.* **2006**, 5743.

(73)   Granifo, J.; Garland, M. T.; Baggio, R. *Inorg. Chem. Commun.* **2004**, *7*, 77.

(74)   Hu, T. L.; Zon, R. Q.; Li, J. R.; Bu, X. H. *Dalton Trans.* **2008**, 1302.

(75)   Breitinger, B. K. In *Coomprehensive Coord. Chem.*; Mccleverty, J., Meyer, T. J., Eds.; Pergamon, 2004; Vol. 6, pp 1254 -1292.

(76)   Ara, I.; Berenguer, J. R.; Eguizábal, E.; Forniés, J.; Lalinde, E.; Martínez, F. *Organometallics* **1999**, *18*, 4344.

(77)   Ara, I.; Berenguer, J. R.; Eguizabal, E.; Forniés, J.; Lalinde, E.; Martín, A.; Martínez, F. *Organometallics* **1998**, *17*, 4578.

(78)   Forniés, J.; Gómez-Saso, M. A.; Lalinde, E.; Martínez, F.; Moreno, M. T. *Organometallics* **1992**, *11*, 2873.

(79)   Winter, M. *www.webelements.com: The Periodic Table on the W. W. W.*; The University of Shefield and Web Elements Ltd., U. K., 2008.

(80)   Yam, V. W.-W.; Pui, Y. L.; Cheung, K.-K. *New J. Chem.* **1999**, *23*, 1163.

(81)   Anjali, K. S.; Pui, Y. L.; Yam, V. W.-W.; Vittal, J. J. *Inorg. Chim. Acta* **2001**, *319*, 57.

(82)   Gou, L.; Wu, Q. R.; Hu, H. M.; Qin, T.; Xue, G. L.; Yang, M. L.; Tang, A. X. *Polyhedron* **2008**, *27*, 1517.

(83)   Holloway, C. E.; Melnik, M. *J. Organomet. Chem.* **1996**, *522*, 167 and references therein.

(84)   Forniés, J.; Martin, A. In *Metal Clusters in Chemistry*; Braunstein, P., Oro, L. A., Raithby, P. R., Eds.; Wiley-VCH: Weinheim, 1999; Vol. 1, p 417.

(85)   Martin, E.; Spendly, C.; Mounford, A. J.; Coles, S. J.; Norton, P. N.; Hughes, D. L.; Hursthouse, M. B.; Lancaster, S. J. *Organometallics* **2008**, *27*, 1436 and references therein.

(86)   Berenguer, J. R.; Lalinde, E.; Torroba, J. *Inorg. Chem.* **2007**, *46*, 9919.

(87)   Ye, B.-H.; Tong, M.-L.; Chen, X.-M. *Coord. Chem. Rev.* **2005**, *249*, 545.

(88)   Nishio, M. In *Weak Hydrogens Bonds*; Atwood, J. L., Steed, J. W., Eds.; Marcel Dekker, Inc.: New York, 2005, p 1576.

(89)   Desiraju, G. R. *Acc. Chem. Res.* **2002**, *35*, 565.

(90)   Shao, P.; Sun, W. *Inorg. Chem.* **2007**, *46*, 8603.

(91)   Steven, C. F. K.; Stephen, S., -Y. C.; Che, C.-M.; Zhu, N. *J. Am. Chem Soc.* **2006**, *128*, 8297.

(92)   Díez, A.; Forniés, J.; García, A.; Lalinde, E.; Moreno, M. T. *Inorg. Chem.* **2005**, *44*, 2443 - 2453.

(93)   Lu, W.; Chan, M. C. W.; Zhu, N.; Che, C.-M.; Li, C.; Hui, Z. *J. Am. Chem Soc.* **2004**, *126*, 7639.

(94)   Lu, W.; Chan, M. C. W.; Zhu, N.; Che, C.-M.; He, Z.; Wong, K.-Y. *Chem. Eur. J.* **2003**, *9*, 6155.

(95)   Berenguer, J. R.; Díez, A.; Fernández, J.; Forniés, J.; García, A.; Gil, B.; Lalinde, E.; Moreno, M. T. *Inorg. Chem.* **2008**, *47*, 7703.

(96)   Nishio, M.; M.Hirota; Umezawa, Y. *The CH/pi Interaction (Evidence, Nature and Consequences)*; Wiley-VCH: New York, 1998.

(97)   Bernechea, M.; Lugan, N.; Gil, B.; Lalinde, E.; Lavigne, G. *Organometallics* **2006**, *25*, 684.

(98)   Nishio, M. *CrystEngComm* **2004**, *6*, 130 and references therein.

(99)   Benito, J.; Berenguer, J. R.; Forniés, J.; Gil, B.; Gómez, J.; Lalinde, E. *Dalton Trans.* **2003**, 4331.

(100)   Suezawa, H.; Yoshida, T.; Umezawa, Y.; Tsuboyama, S. T.; Nishio, M. *Eur. J. Inorg. Chem.* **2002**, 3148.

(101)   Braga, D.; Grepion, F.; Tedesco, E. *Organometallics* **1998**, *17*, 2669.

(102)   Sreerama, S. G.; Pal, S. *Inorg. Chem.* **2005**, *44*, 6299.

(103)   Desiraju, G. R. *Chem. Commun.* **2005**, 2995.

(104)   Chopra, D.; Thiruvenkatam, V.; Manjunath, S. G.; Guru Row, T. N. *Cryst. Growth. Des.* **2007**, *7*, 868.

(105)   Reichenbächer, K.; Süss, H. I.; Hulliger, J. *Chem. Soc. Rev.* **2005**, *34*, 22.

(106)   Berenguer, J. R.; Forniés, J.; Lalinde, E.; Martín, A.; Serrano, B. *J. Chem. Soc., Dalton Trans.* **2001**, 2926 and references therein.

(107)   Dunitz, J. D.; Taylor, R. *Chem. Eur. J* **1997**, *3*, 89.

(108)   Berenguer, J. R.; Forniés, J.; Gómez, J.; Lalinde, E.; Moreno, M. T. *Organometallics* **2001**, *20*, 4847 and references therein.

(109)   Benito, J.; Berenguer, J. R.; Forniés, J.; Gil, B.; Gómez, J.; Lalinde, E. *Dalton Trans.* **2003**, 4331.

(110)   Gagnon, K.; Aly, S. M.; Brisach-Withmeyer, A.; Bellows, D.; Bérubé, J. F.; Caron, L.; Abd-El-Aziz, A. S.; Fortin, D.; Harvey, P. D. *Organometallics* **2008**, *27*, 2201.

(111)   Cooper, T. M.; Krein, D. M.; Burke, A. R.; McLean, D. G.; Rogers, J. E.; Slagle, J. E.; Fleitz, P. A. *J. Phys. Chem. B* **2006**, 4369.

(112)   Díez, A.; Fernández, J.; Lalinde, E.; Moreno, M. T.; Sánchez, S. *Dalton Trans.* **2008**, 4926.

(113)   Wang, S.; Bai, D. R. *Organometallics* **2006**, *25*, 1517.

(114)   Ferraudi, G. J. *Elements of Inorganic Photochemistry*; John Wiley and sons: New York, 1988.

(115)   Beljonne, D.; Wittmann, H. F.; Köhler, A.; Graham, S.; Younus, M.; Lewis, J.; Raithby, P. R.; Khan, M. S.; Friend, R. H.; Bredas, J. L. *J. Chem. Phys.* **1996**, *105*, 3868.

(116)   Ksenija, H.-G.; Chiriuiga, I.; Abboud, K. A.; Schanze, K. S. *J. Phy. Chem.* **2004**, *108*, 4969.

(117)   Glusac, K.; Erkan Köse, M.; Jiang, H.; Schanze, K. S. *J. Phy. Chem.* **2007**, *111*, 929.

(118)   Kim, K. Y.; Liu, S.; Köse, M. E.; Schanze, K. S. *Inorg. Chem.* **2006**, *45*, 2509.

(119)   de Quadras, L.; Shelton, A. H.; Kuhn, H.; Hampel, F.; Schanze, K. S.; Gladysz, J. A. *Organometallics* **2008**, *27*, 4979.

Table 1. Crystallographic Data for **1a**·$(CH_3)_2CO$, **2a**·$(CH_3)_2CO$·$0.75H_2O$, **3a**·$(CH_3)_2CO$, **4a**·$2(CH_3)_2CO$, **4b**·$3(CH_3)_2CO$·H_2O, **6b**·$2(CH_3)_2CO$.

	1a·$(CH_3)_2CO$	**2a**·$(CH_3)_2CO$·$0.75H_2O$	**3a**·$(CH_3)_2CO$
Empirical formula	C51 H32 Cd F10 N4 O Pt	C55 H40 Cd F10 N4 O1.75 Pt	C55 H32 Cd F10 N4 O Pt
F_w	1214.30	1282.40	1262.34
T (K)	293(2)	173(1)	293(2)
crystal system, space group	Triclinic; P-1	Monoclinic, P21/n	Triclinic, P-1
a(Å)	11.4895(2)	15.3110(2)	11.1692(2)
b(Å)	12.1929(3)	19.9720(3)	12.4612(2)
c(Å)	19.8162(5)	17.0120(3)	19.4842(5)
α(deg)	91.2460(10)	90	92.6990(10)
β(deg)	91.6520(10)	97.2920(10)	102.5990(10)
γ(deg)	116.060(2)	90	116.275(2)
volume (A^3)	2490.96(10)	5160.05(14)	2340.91(8)
Z	2	4	2
D_{calcd} (Mg/m^3)	1.619	1.651	1.791
absorption coefficient (mm^{-1})	3.309	3.201	3.525
F(000)	1180	2512	1228
θ range for data collection (deg)	4.12 to 25.68	1.97 to 26.37	2.06 to 27.97
no of data / restraints / params	9380 / 0 / 615	10548 / 7 / 652	11000 / 0 / 651
goodness-of-fit on F^2[a]	1.037	1.035	1.015
final R indices [I>2σ(I)][a]	R1 = 0.0446, wR2 = 0.1003	R1 = 0.0389, wR2 = 0.0969	R1 = 0.0434, wR2 = 0.1052
R indices (all data)[a]	R1 = 0.0673, wR2 = 0.1075	R1 = 0.0551, wR2 = 0.1045	R1 = 0.0550, wR2 = 0.1132
largest diff peak and hole (e.$Å^{-3}$)	1.017 and -1.012	1.550 and -1.106	1.380 and -2.390

[a] $R1 = \Sigma(|F_o| - |F_c|)/\Sigma|F_o|$; wR2 = $[\Sigma w(F_o^2 - F_c^2)^2/\Sigma wF_o^2]^{1/2}$; goodness of fit = $\{\Sigma[w(F_o^2 - F_c^2)^2]/(N_{obs} - N_{param})\}^{1/2}$; $w = [\sigma^2(F_o) + (g_1P)^2 + g_2P]^{-1}$; $P = [max(F_o^2; 0 + 2F_c^2]/3$.

Table 1. Continue.

	4a·2 (CH$_3$)$_2$CO	**4b·3(CH$_3$)$_2$CO·H$_2$O**	**6b·2(CH$_3$)$_2$CO**
Empirical formula	C49 H33 Cd F10 N3 O2 Pt	C99 H68 Cd2 F20 N6 O4 Pt2	C56 H42 Cd F10 N4 O2 Pt
F_w	1193.27	2400.57	1300.43
T (K)	293(2)	173(1)	223(1)
crystal system, space group	Triclinic, P -1	Triclinic, P-1	Monoclinic, Cc
a(Å)	12.5370(2)	15.1965(2)	16.9220(3)
b(Å)	14.1520(2)	15.5331(2)	25.2140(6)
c(Å)	15.6139(3)	19.7826(3)	13.8280(3)
α(deg)	116.1620(10)	83.9210(10)	90
β(deg)	92.1180(10)	87.1790(10)	107.598(2)
γ(deg)	113.7240(10)	76.5470(10)	90
volume (A^3)	2197.53(6)	4514.53(11)	5623.9(2)
Z	2	2	4
D_{calcd} (Mg/m^3)	1.803	1.766	1.536
absorption coefficient (mm^{-1})	3.750	3.651	2.938
F(000)	1160	2336	2552
θ range for data collection (deg)	3.56 to 27.48	1.38 to 25.68	3.49 to 26.37
no of data / restraints / params	10058 / 0 / 599	16860 / 2 / 1196	10995 / 9 / 656
goodness-of-fit on F$^{2[a]}$	1.004	1.065	1.032
final R indices [I>2σ(I)][a]	R1 = 0.0378, wR2 = 0.0744	R1 = 0.0586, wR2 = 0.1573	R1 = 0.0444, wR2 = 0.1180
R indices (all data)[a]	R1 = 0.0577, wR2 = 0.0786	R1 = 0.0801, wR2 = 0.1775	R1 = 0.0497, wR2 = 0.1223
largest diff peak and hole (e.Å^{-3})	1.296 and -1.415	1.832 and -3.073	1.202 and -1.172

[a] $R1 = \Sigma(|F_o| - |F_c|)/\Sigma|F_o|$; w$R2 = [\Sigma w(F_o^2 - F_c^2)^2/\Sigma wF_o^2]^{1/2}$; goodness of fit = $\{\Sigma[w(F_o^2 - F_c^2)^2]/(N_{obs} - N_{param})\}^{1/2}$; $w = [\sigma^2(F_o) + (g_1P)^2 + g_2P]^{-1}$; $P = [\max(F_o^2; 0 + 2F_c^2]/3$.

Table 2: Selected Bond Lengths [Å] and Angles [deg] for Complexes [*cis*-Pt(C$_6$F$_5$)$_2$(C≡CPh)$_2$Cd(bpy)$_2$]·(CH$_3$)$_2$CO **1a**·(CH$_3$)$_2$CO, [*cis*-Pt(C$_6$F$_5$)$_2$(C≡CPh)$_2$Cd(dmbpy)$_2$]·(CH$_3$)$_2$CO·0.75H$_2$O **2a**·(CH$_3$)$_2$CO·0.75H$_2$O, [*cis*-Pt(C$_6$F$_5$)$_2$(C≡CPh)$_2$Cd(phen)$_2$]·(CH$_3$)$_2$CO **3a**·(CH$_3$)$_2$CO, and [*cis*-Pt(C$_6$F$_5$)$_2$(C≡CPh)$_2$Cd(trpy)]·2(CH$_3$)$_2$CO, **4a**·2(CH$_3$)$_2$CO.

		1a·(CH$_3$)$_2$CO	**2a**·(CH$_3$)$_2$CO·0.75H$_2$O	**3a**·(CH$_3$)$_2$CO	**4a**·2(CH$_3$)$_2$CO
Pt-Cd	Pt(1)-Cd(1)	3.1087(5)	3.1163(4)	3.0990(4)	2.9998(3)
Pt-C$_\alpha$	Pt(1)-C(13)	2.041(6)	2.027(5)	2.014(5)	2.013(4)
	Pt(1)-C(21)	2.036(7)	2.025(5)	2.032(5)	2.008(4)
Pt-C$_{ipso}$(C$_6$F$_5$)	Pt(1)-C(1)	2.061(6)	2.060(5)	2.075(5)	2.061(4)
	Pt(1)-C(7)	2.074(6)	2.068(5)	2.069(5)	2.052(4)
C$_\alpha$-C$_\beta$	C(13)-C(14)	1.201(8)	1.196(7)	1.212(7)	1.208(5)
	C(21)-C(22)	1.191(8)	1.216(7)	1.200(7)	1.220(6)
Cd-C$_\alpha$	Cd(1)-C(13)	2.527(5)	2.497(5)	2.417(5)	2.446(4)
	Cd(1)-C(21)	2.427(6)	2.478(5)	2.554(5)	2.410(4)
Cd- C$_\beta$	Cd(1)-C(14)	2.915(8)	2.896(5)	2.911(6)	2.851(5)
	Cd(1)-C(22)	2.917(7)	2.841(5)	2.913(7)	2.782(6)
Cd-N	Cd(1)-N(1)	2.318(5)	2.341(4)	2.375(4)	2.334(3)
	Cd(1)-N(2)	2.365(5)	2.412(4)	2.380(4)	2.335(3)
	Cd(1)-N(3)	2.381(5)	2.368(4)	2.336(4)	2.382(3)
	Cd(1)-N(4)	2.365(5)	2.340(4)	2.382(4)	
Cd-O	Cd(1)-O(1)				2.461(3)
C$_\alpha$-Pt-C$_\alpha$	C(13)-Pt(1)-C(21)	98.0(2)	93.8(2)	97.5(2)	95.5(2)
Pt-C$_\alpha$-C$_\beta$	Pt(1)-C(13)-C(14)	174.2(6)	176.5(4)	170.3(5)	177.5(4)
	Pt(1)-C(21)-C(22)	170.2(6)	178.7(4)	174.3(5)	178.0(4)
C$_\alpha$-C$_\beta$-Cγ	C(13)-C(14)-C(15)	178.6(7)	175.3(5)	172.0(6)	178.9(4)
	C(21)-C(22)-C(23)	172.6(7)	174.9(5)	176.5(6)	172.4(4)
C$_\alpha$-Cd-C$_\alpha$	C(13)-Cd(1)-C(21)	76.7(2)	73.0(2)	75.3(2)	75.6(1)

Table 2: Continue

Cα-Cd-N					
	C(13)-Cd(1)-N(1)	96.2(2)	110.0(2)	93.9(2)	95.1(1)
	C(13)-Cd(1)-N(2)	166.3(2)	173.4(2)	164.0(2)	104.7(1)
	C(13)-Cd(1)-N(3)	100.5(2)	97.9(2)	102.7(2)	94.5(1)
	C(13)-Cd(1)-N(4)	92.9(2)	93.5(2)	105.3(2)	
	C(21)-Cd(1)-N(1)	100.7(2)	93.5(2)	90.4(2)	121.5(1)
	C(21)-Cd(1)-N(2)	102.8(2)	100.4(2)	101.8(2)	168.1(1)
	C(21)-Cd(1)-N(3)	166.3(2)	170.4(2)	91.7(2)	99.1(1)
	C(21)-Cd(1)-N(4)	97.8(2)	106.6(2)	162.4(2)	
Cα-Cd-O	C(13)-Cd(1)-O(1)				153.9(1)
	C(21)-Cd(1)-O(1)				87.4(1)

Table 3: Selected Bond Lengths [Å] and Angles [deg] for **4b**·3(CH$_3$)$_2$CO·H$_2$O

	4b·(CH$_3$)$_2$CO		**4b**·H$_2$O	
Pt-Cd	Pt(1)-Cd(1)	3.0095(6)	Pt(2)-Cd(2)	3.0320(6)
Pt-C$_\alpha$	Pt(1)-C(1)	2.017(8)	Pt(2)-C(46)	2.000(8)
	Pt(1)-C(10)	2.002(8)	Pt(2)-C(55)	2.034(8)
Pt-C$_{ipso}$(C$_6$F$_5$)	Pt(1)-C(19)	2.066(8)	Pt(2)-C(64)	2.051(8)
	Pt(1)-C(25)	2.047(7)	Pt(2)-C(70)	2.062(9)
C$_\alpha$-C$_\beta$	C(1)-C(2)	1.213(11)	C(46)-C(47)	1.217(11)
	C(10)-C(11)	1.224(10)	C(55)-C(56)	1.190(11)
Cd-C$_\alpha$	Cd(1)-C(1)	2.463(7)	Cd(2)-C(46)	2.491(7)
	Cd(1)-C(10)	2.355(7)	Cd(2)-C(55)	2.405(8)
Cd- C$_\beta$	Cd(1)-C(2)	2.948(8)	Cd(2)-C(47)	2.949(7)
	Cd(1)-C(11)	2.740(9)	Cd(2)-C(56)	2.792(9)
Cd-N	Cd(1)-N(1)	2.346(6)	Cd(2)-N(4)	2.338(6)
	Cd(1)-N(2)	2.317(6)	Cd(2)-N(5)	2.338(6)
	Cd(1)-N(3)	2.329(6)	Cd(2)-N(6)	2.353(6)
Cd-O	Cd(1)-O(1)	2.652(7)	Cd(2)-O(2)	2.398(6)
C$_\alpha$-Pt-C$_\alpha$	C(1)-Pt(1)-C(10)	94.9(3)	C(46)-Pt(2)-C(55)	94.7(3)
Pt-C$_\alpha$-C$_\beta$	Pt(1)-C(1)-C(2)	172.1(6)	Pt(2)-C(46)-C(47)	175.9(6)
	Pt(1)-C(10)-C(11)	178.3(7)	Pt(2)-C(55)-C(56)	178.3(7)
C$_\alpha$-C$_\beta$-Cγ	C(1)-C(2)-C(3)	174.1(8)	C(46)-C(47)-C(48)	175.9(8)
	C(10)-C(11)-C(12)	170.2(8)	C(55)-C(56)-C(57)	169.9(8)
C$_\alpha$-Cd-C$_\alpha$	C(1)-Cd(1)-C(10)	75.8(3)	C(46)-Cd(2)-C(55)	74.6(3)
C$_\alpha$-Cd-N	C(1)-Cd(1)-N(1)	99.7(2)	C(46)-Cd(2)-N(4)	97.6(2)
	C(1)-Cd(1)-N(2)	112.7(2)	C(46)-Cd(2)-N(5)	109.8(2)
	C(1)-Cd(1)-N(3)	97.3(2)	C(46)-Cd(2)-N(6)	95.0(2)
	C(10)-Cd(1)-N(1)	99.7(2)	C(55)-Cd(2)-N(4)	102.9(2)
	C(10)-Cd(1)-N(2)	170.5(2)	C(55)-Cd(2)-N(5)	172.0(2)
	C(10)-Cd(1)-N(3)	113.4(2)	C(55)-Cd(2)-N(6)	118.0(2)
C$_\alpha$-Cd-O	C(1)-Cd(1)-O(1)	168.5(3)	C(46)-Cd(2)-O(2)	164.8(2)
	C(10)-Cd(1)-O(1)	96.7(3)	C(55)-Cd(2)-O(2)	94.1(2)

Table 4: Selected Bond Lengths [Å] and Angles [deg] for complex [*trans*-Pt(C$_6$F$_5$)$_2$(C≡CTol)$_2$Cd(bpy)$_2$]·2(CH$_3$)$_2$CO **6b**·2(CH$_3$)$_2$CO.

Pt(1)-Cd(1)	2.8966(6)	Pt(1)-C(1)	2.027(10)
Pt(1)-C(10)	1.981(12)	Pt(1)-C(19)	2.079(8)
Pt(1)-C(25)	2.057(8)	C(1)-C(2)	1.230(17)
C(10)-C(11)	1.226(16)	Cd(1)-C(1)	2.372(10)
Cd(1)-C(2)	2.893(11)	Cd-N(1)	2.362(6)
Cd-N(2)	2.405(7)	Cd-N(3)	2.327(7)
Cd-N(4)	2.338(7)		
C(2)-C(1)-Pt(1)	172.6(7)	C(11)-C(10)-Pt(1)	176.8(10)
C(1)-C(2)-C(3)	177.1(10)	C(10)-C(11)-C(12)	175.4(12)
N(1)-Cd(1)-N(2)	69.6(2)	N(2)-Cd(1)-N(4)	87.5(3)
N(3)-Cd(1)-N(4)	70.1(3)	N(1)-Cd(1)-N(3)	98.8(3)
N(2)-Cd(1)-N(3)	94.9(3)	N(4)-Cd(1)-Pt(1)	90.8(2)
C(1)-Cd(1)-N(3)	107.0(3)	C(1)-Cd(1)-N(4)	110.2(3)
C(1)-Cd(1)-N(1)	95.4(2)	C(1)-Cd(1)-N(2)	155.3(3)

Table 5: Absorption Data for **1b** - **6b** and **5a** in CH$_2$Cl$_2$ (5 x 10^{-5} M).

Compound	Absorption /nm (10^3 ε/M^{-1} cm^{-1})
1b	227s*h* (42.5), 245 (45.3), 286 (48.6), 294 (45), 307s*h* (35.8)[a]
2b	230s*h* (43.2), 262 (61.3), 303 (57.3), 315s*h* (45.2)[a]
3b	237 (58.8), 258s*h* (57.8), 274 (61.3), 292s*h* (47.0), 311 (20.1)[a]
4b	233 (50.5), 268 (22.6), 307 (21.9), 321 (20.6), 334 (17.7)
5a	232 (28.2), 295 (30.8), 334 (30.3), 342*sh* (28.9)
5b	230 (25.3), 293 (32.0), 331 (31.3), 338s*h* (30.0)
6b	228s*h* (30.8), 246 (34.7), 295 (36.8), 307s*h* (28.1), 336 (12.3)[a]

[a]Tail over 360 nm

Table 6. Photophysical Data for Complexes **1 – 6** in Solid State.

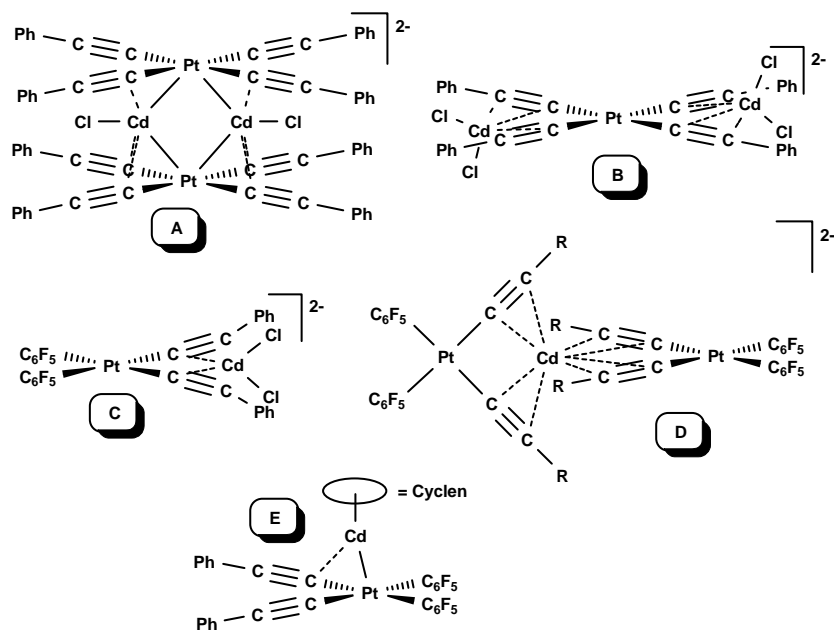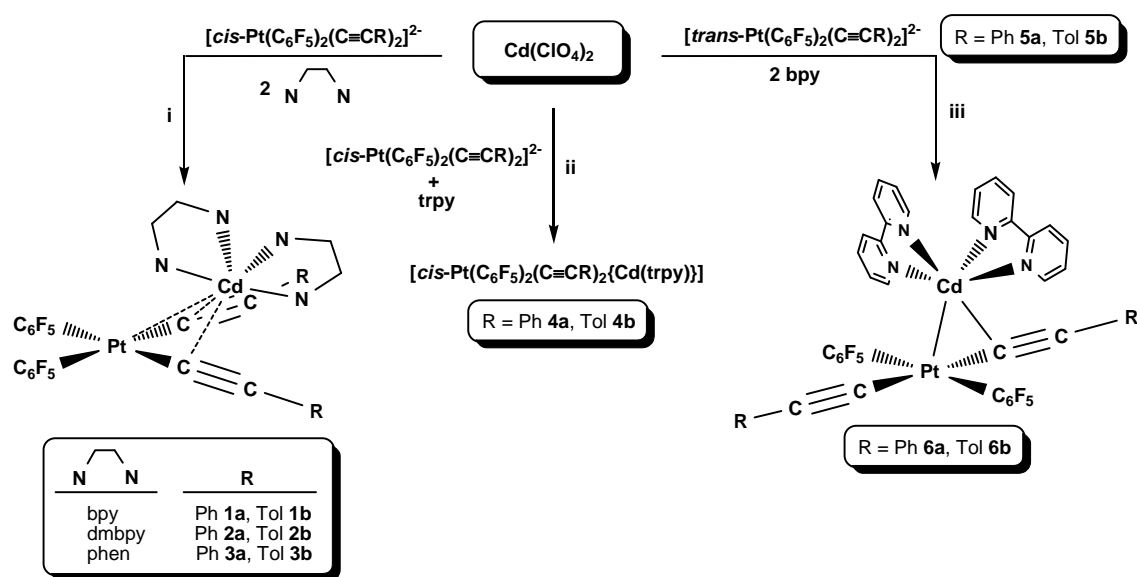| Compound	(T/K)	λ_{max}^{em} /nm	τ
1a	298	441*sh*, 475*sh*, 508*sh*, 534$_{max}$, 570*sh* (λ_{ex} 370)	9 μs (λ_{em} 534)
	77	443*sh*, 472$_{max}$, 504 (λ_{ex} 320-360)	3.5 (68%), 0.3 (32%) ms (λ_{em} 472)
1b	298	450*sh*, 495$_{max}$, 517 (λ_{ex} 325-360)	32 μs (λ_{em} 517)
	77	453, 483, 521*sh* (λ_{ex} 320-420)	81 μs (λ_{em} 453)
			152 (14%), 68 (86%) μs (λ_{em} 483)
2a	298[a]	450$_{max}$, 467*sh*, 515*sh* (λ_{ex} 370)	8 μs (λ_{em} 452)
	77	461$_{max}$, 501*sh* (λ_{ex} 350-380)	1.4 (84%), 19.2 (16%) ms (λ_{em} 461)
2b	298	450*sh*, 495$_{max}$, 519 (λ_{ex} 335-365)	43 μs (λ_{em} 495)
	77	450*sh*, 486$_{max}$, 518*sh*, 565*sh* (λ_{ex} 330-415)	257 (63%), 83 (37%) μs (λ_{em} 450)
			373 (92%), 65 (8%) μs (λ_{em} 485)
3a	298[a]	485*sh*, 495*sh*, 529 (λ_{ex} 370)	9 μs (λ_{em} 529)
	77[a]	485*sh*, 523 (λ_{ex} 366)	26.1 (47%), 0.83 (53%) ms (λ_{em} 523)
3b	298	440*sh*, 473*sh*, 505$_{max}$, 527*sh* (λ_{ex} 370-400)	14 μs (λ_{em} 505)
	77	440*sh*, 492$_{max}$, 521 (λ_{ex} 330-425)	1.1 (4%), 0.12 (96%) ms (λ_{em} 492)
4a	298	493$_{max}$, 520 (λ_{ex} 368-445)	14 μs (λ_{em} 493)
	77	460*sh*, 485, 523, 560*sh* (λ_{ex} 360)	30.2 (55%), 0.6 (45%) ms (λ_{em} 485)
4b	298	527 (λ_{ex} 360-420)	12 μs (λ_{em} 527)
	77	517 (λ_{ex} 330-400)	1.1 (12%), 0.05 (88%) ms (λ_{em} 515)
5a	298	460$_{max}$, 480, 503*sh* (λ_{ex} 370)	16 μs (λ_{em} 460)
	77	457$_{max}$, 478, 492, 504 (λ_{ex} 360)	16 μs (λ_{em} 457)
5b	298	465$_{max}$, 480s*h*, 510s*h* (λ_{ex} 380)	17 μs (λ_{em} 465)
	77	460$_{max}$, 480, 492, 505 (λ_{ex} 367)	18 μs (λ_{em} 460)
6a	298	No emissive	
	77	448$_{max}$, 495 (λ_{ex} 370)	13 μs (λ_{em} 448)
6b	298	No emissive	
	77	455$_{max}$, 520$_{max}$, (λ_{ex} 370)	14 μs (λ_{em} 455); 11 μs (λ_{em} 520)

[a] Weak emission

Chart 1

Scheme 1

Figure Captions:

Figure 1: Molecular structure of complex [*cis*-Pt(C$_6$F$_5$)$_2$(C≡CPh)$_2$Cd(bpy)$_2$] **1a** with the ellipsoids drawn at 50% probability level and hydrogen atoms omitted for clarity.

Figure 2: Molecular structure of the adduct [*cis*-Pt(C$_6$F$_5$)$_2$(C≡CPh)$_2$Cd(trpy){(CH$_3$)$_2$CO}] (**4a·**(CH$_3$)$_2$CO), with the ellipsoids drawn at 50% probability level and hydrogen atoms omitted for clarity.

Figure 3: (**a**) Molecular structure of (**a**) the adduct [*cis*-Pt(C$_6$F$_5$)$_2$(C≡CTol)$_2$Cd(trpy){(CH$_3$)$_2$CO}] (**4b·**(CH$_3$)$_2$CO) and (**b**) the adduct [*cis*-Pt(C$_6$F$_5$)$_2$(C≡CTol)$_2$Cd(trpy)(OH$_2$)] (**4b·**(OH$_2$)). Ellipsoids are drawn at 50% probability level and hydrogen atoms omitted for clarity.

Figure 4: (**a**) Molecular structure of complex [*trans*-Pt(C$_6$F$_5$)$_2$(C≡CTol)$_2$Cd(bpy)$_2$] **6b** with the ellipsoids drawn at 50% probability level and hydrogen atoms omitted for clarity. (**b**) Detail of the intra- and intermolecular ππ stacking observed along the *c* axis for **6b.** Molecules are simplified for clarity.

Figure 5: Absorption spectra of **1b** (dark line), **2b** (light line) and **3b** (dashed line) in CH$_2$Cl$_2$ (5 x 10^{-5} M).

Figure 6: Absorption spectra of **5b** (dark line) and **6b** (light line) in CH$_2$Cl$_2$ (5 x 10^{-5} M).

Figure 7: Normalized emission spectra for crystalline samples of **1b**, **2b**, **3b** and **4b** at different temperatures.

Figure 8: Normalized emission spectra of **1b**, **2b**, **3b**, **4b** in 2-MeTHF glasses (5 x 10^{-4} M) at 77K.

Figure 9: Normalized site-selectivity dual emission and excitation spectra of **5b** in CH$_2$Cl$_2$ glass (5 x 10^{-4} M) at 77K.

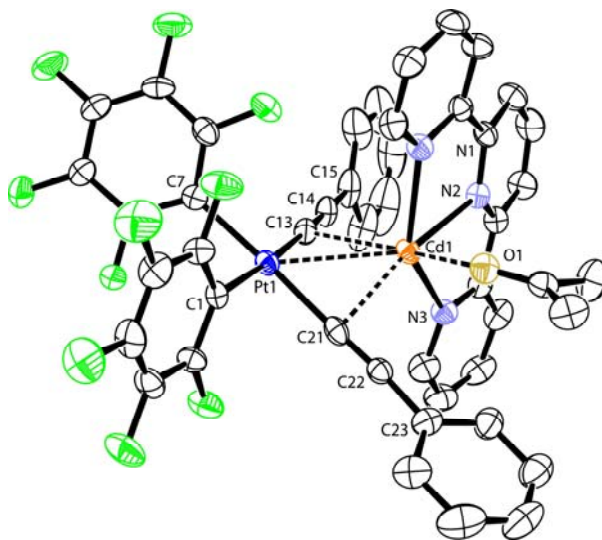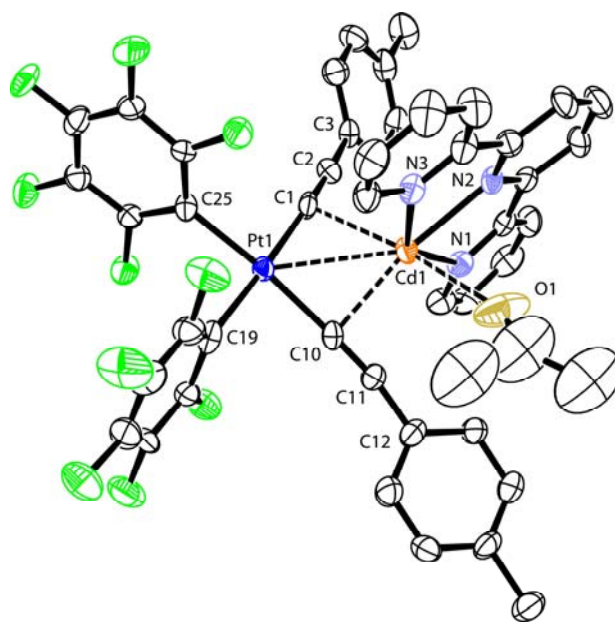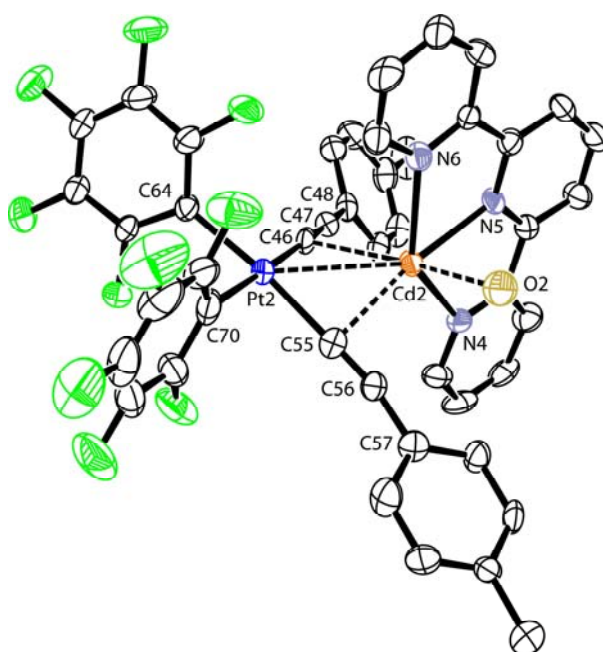**Figure 10:** Normalized emission and excitation spectra of solid **6b** at 77K.
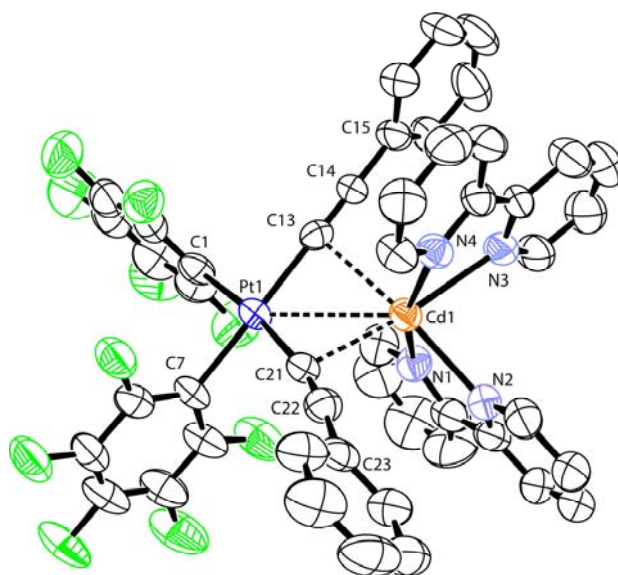
Figure 1

Figure 2

(a)

(b)

Figure 3
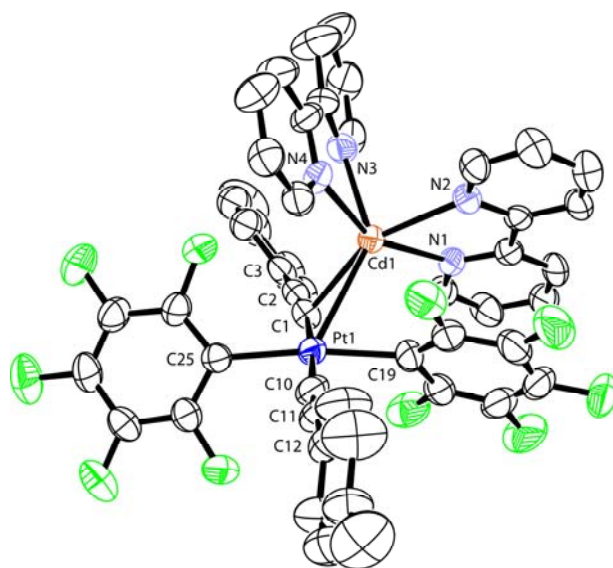
(a)
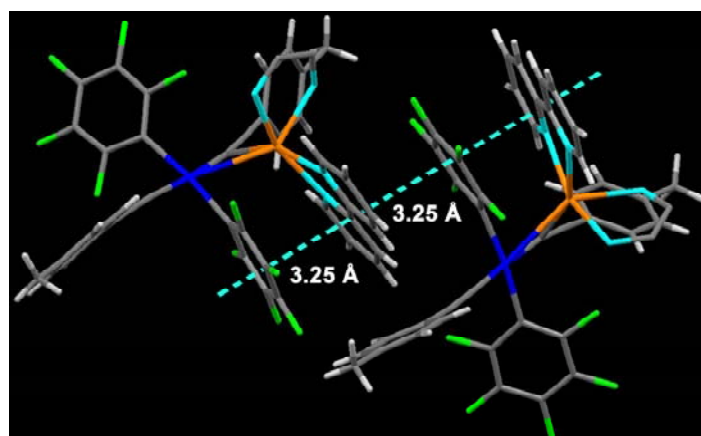
(b)

Figure 4
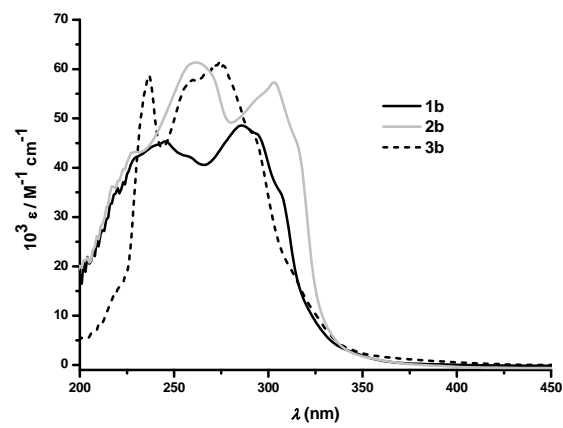
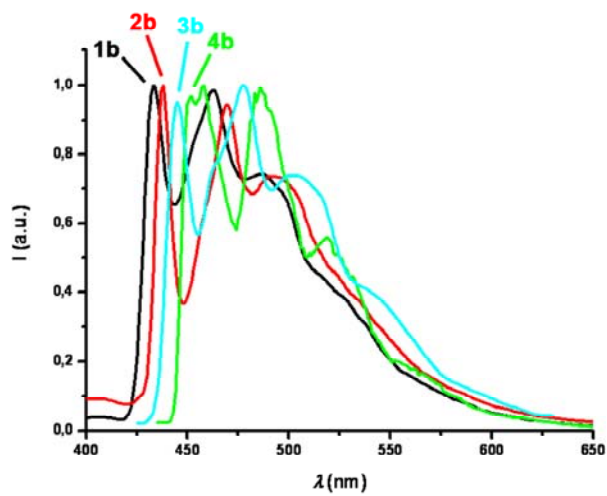**Figure 5**
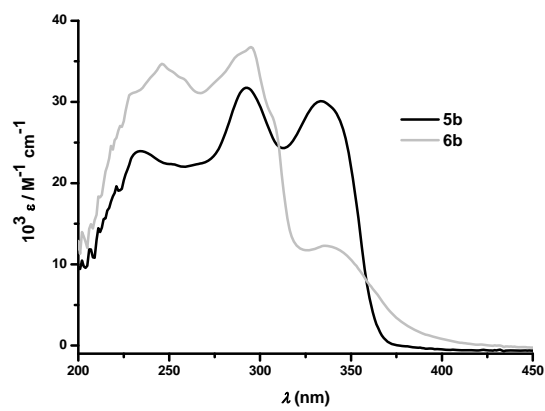
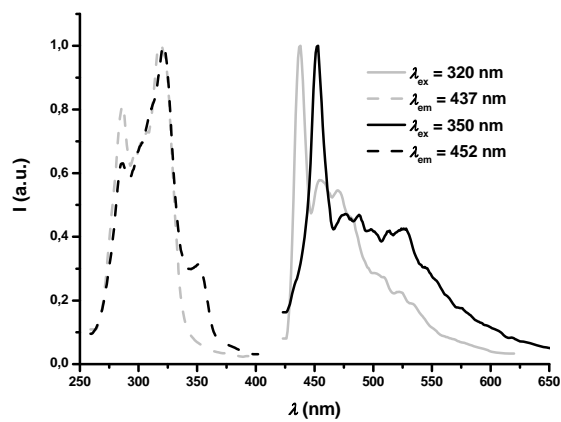
Figure 6
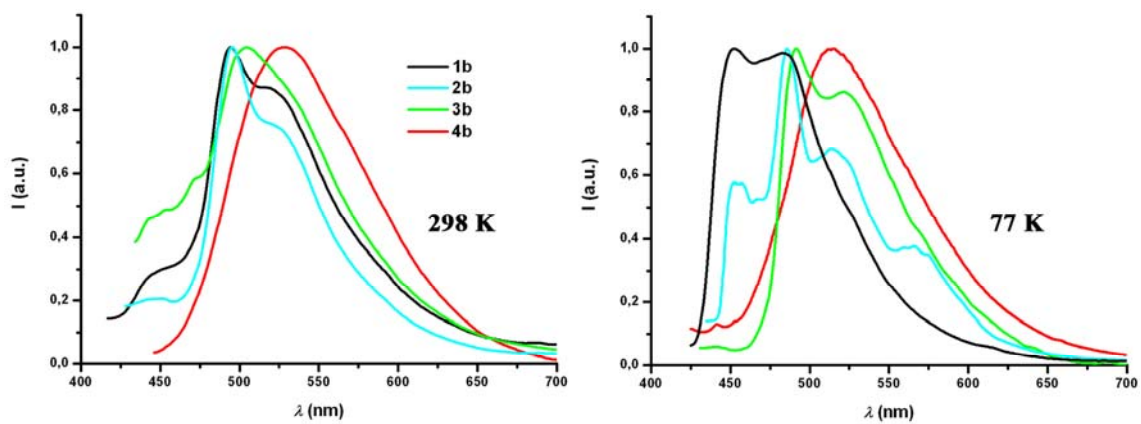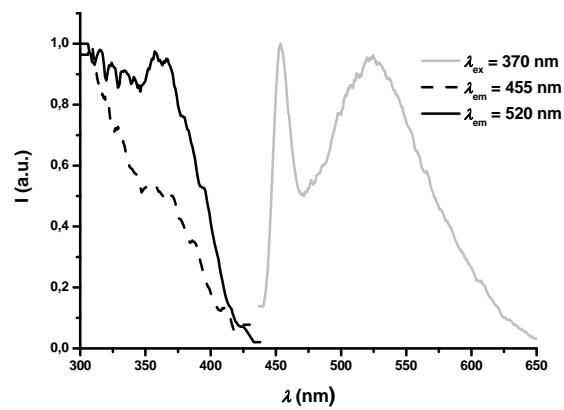
Figure 7

Figure 8

Figure 9

Figure 10

"for Table of Contents use only"

Self-Assembly of Luminescent Alkynyl-Based Platinum-Cadmium Complexes Containing Auxiliary Diimine or Terpyridine Ligands.

Jesús R. Berenguer,*† Belén Gil,† Julio Fernández,† Juan Forniés‡ and Elena Lalinde*†

Reaction of different "Cd(diimine)$_2$$^{2+}$" or "Cd(triimine)$^{2+}$" fragments with *cis-* or *trans-*dianionic bis(alkynyl) platinate substrates $[Pt(C_6F_5)_2(C\equiv CR)_2]^{2-}$ leads to the generation of novel bimetallic neutral Platinum-Cadmium derivatives. These complexes show PL in the blue-green zone, which is affected by the structure and the media.